Metabolomic Profile Associated With Hyperglycemia And Chronic Diseases And Metabolic Homeostasis Derangement In Critical Illness: Post-hoc metabolomic cohort study of the VITdAL-ICU Trial

Metabolomic Profile Associated With Hyperglycemia And Chronic Diseases And Metabolic Homeostasis Derangement In Critical Illness: Post-hoc metabolomic cohort study of the VITdAL-ICU Trial

By

Sigma Hossain, MBBS, MSc, MSc, MPhil, MPH

A Dissertation Submitted to the Faculty of Harvard Medical School in Partial Fulfillment of the Requirements for the Degree of Master of Medical Sciences in Clinical Investigation (MMSCI)

Harvard University
Boston, Massachusetts
May 3rd , 2023

Thesis Committee Members:
MMSCI Program Directors: Ajay K. Singh, Finnian McCausland
Primary Mentor: Kenneth B. Christopher
MMSCI Program Representative: Gearoid M. McMahon
External Content Advisor: Martin Ingi Sigurdsson
Independent External Expert: Olav Rooijackers

Area of Concentration: Metabolomics/Critical Care Outcomes

I have reviewed this thesis. It represents work done by the author under my guidance/supervision.

Primary Mentor: Kenneth B. Christopher, MD, SM

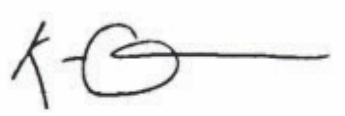

_____

TABLE OF CONTENTS

MANUSCRIPT 2:

Chronic Diseases and Metabolic Homeostasis Derangement in Critical Illness: A Post-hoc Metabolomics cohort study

ACKNOWLEDGMENT

First and foremost, I would like to express my sincere gratitude and appreciation to my mentor, Dr. Kenneth B. Christopher, for his tenacious and invaluable guidance over the past two years. In addition to imparting valuable practical knowledge on conceptualizing and carrying out studies, he did so with the utmost positivity and patience. Dr. Kenneth's ongoing assistance, inspiration, and direction are greatly appreciated. Without his help, this project would not have been possible.

Next, I would like to express my gratitude to Dr. Singh, Dr. McCausland, and the faculty members of this program, Dr. McGrath, Dr. Adam, and Dr. Perez Chada, who have provided me with this wonderful opportunity and unwavering support over the past two years. Furthermore, I am indebted to Dr. Gearoid M. McMahon, Dr. Martin Ingi Sigurdsson, and Dr. Olav Rooijackers for their encouragement and insightful comments. In addition, I would like to thank Ms. Cacioppo and Gallagher for coordinating the program's courses and related activities.

I'd like to thank Dr. Karin Amrein for her contributions to the VITdAL-ICU trial and Dr. Jessica A. Lasky-Su for her insightful advice regarding metabolomics.

I appreciate my dad, Noor Hossain, for always being there for me.

Last but not least, I'd like to thank Mofazzal, my husband, and my children, Ayan, and Areeba, for all the love, encouragement, and support they've given me over the years.

Sigma Hossain

OVERVIEW

Critical illnesses contribute to the maximum morbidity and mortality of hospitalized patients. Critical illness often results in the loss of metabolic homeostasis, characterized by the severe disruption of various metabolic processes, including energy production and utilization. Despite significant advancements in care for critically ill patients (1,2), approximately 500000 patients (one in five) die in the ICU each year in the USA (3). Metabolomics can provide a comprehensive technique for understanding an organism's phenotype as metabolites indicate cellular and gene activity.

Manuscript 1: Regardless of the patient's diabetes status, hyperglycemia has been associated with poor clinical outcomes in critically ill patients. Acute hyperglycemia impairs innate immunity, despite proinflammatory changes (4). Early metabolomic studies in critical illness showed illness severity and predicted outcomes. However, no existent study has defined the metabolic response to hyperglycemia in the critically ill. We hypothesize that hyperglycemia is associated with metabolism differences related to innate immunity in critically ill patients.

Manuscript 2: Critically ill patients often have chronic medical conditions affecting the severity of the acute illness, treatment, and outcomes. Plasma metabolomics studies in critical illness show a consistent alteration of metabolism linked to acute illness severity and outcome prediction. But the importance of energy utilization pathways among critically ill patients with comorbidities is unknown. Therefore, we hypothesized that a higher chronic disease burden, as assessed by the updated Charlson Comorbidity Index (uCCI), is associated with differential energy utilization pathways in critically ill adult patients.

References

1. Zimmerman JE, Kramer AA, Knaus WA (2013) Changes in hospital mortality for United States intensive care unit admissions from 1988 to 2012. Crit Care 17: R81.

2. Li G, Malinchoc M, Cartin-Ceba R, Venkata CV, Kor DJ, et al. (2011) Eight-Year Trend of Acute Respiratory Distress Syndrome. American Journal of Respiratory and Critical Care Medicine 183: 59–66.

3. Angus DC, et al., Use of intensive care at the end of life in the United States: an epidemiologic study. Crit Care Med. Mar;32(3):638-43. 2004 doi: 10.1097/01.ccm.0000114816.62331.08. PMID: 15090940.

4. Turina M, Fry DE, Polk Jr HC. Acute hyperglycemia and the innate immune system: clinical, cellular, and molecular aspects. Critical care medicine. 2005 Jul 1;33(7):1624-33.

Manuscript 1

The Metabolomics of Elevated Serum Glucose in Critical Illness: A Post-hoc Metabolomics cohort study

Authors: Sigma Hossain, MBBS, MSc, MSc, MPhil, MPH[1,4], Karin Amrein, MD, MSc[2], Jessica A. Lasky-Su, ScD[3], Kenneth B. Christopher, MD, SM[3,4]

Affiliations:

1. Harvard Medical School, Boston, USA
2. Division of Endocrinology and Diabetology, Medical University of Graz, Graz, Austria
3. Jessica A. Lasky-Su, ScD, Channing Division of Network Medicine, Brigham and Women's Hospital, USA
4. Division of Renal Medicine, Channing Division of Network Medicine, Brigham and Women's Hospital, USA

Corresponding Author: Kenneth B. Christopher, MD, SM, Division of Renal Medicine, Channing Division of Network Medicine, Brigham, and Women's Hospital, 75 Francis Street, Boston, MA 02115 USA. E-mail: kbchristopher@bwh.harvard.edu Tel: 617-272-0535

Acknowledgment: This manuscript is dedicated to the memory of our dear friend and colleague Nathan Edward Hellman, MD, Ph.D.

Author's contributions: Conceptualization: S.H., K.A., J.L-S., K.C.; Methodology: S.H., K.A., J.L-S., K.C.; Software: J.L-S., K.C.; Formal analysis: S.H., K.C.; Investigation: K.A., K.C.: Resources: K.A., J.L-S., K.C.; Data Curation: S.H., K.A., J.L-

S., K.C.; Writing-Original Draft: S.H., K.A., J.L-S., K.C.; Writing- Review & Editing: S.H., K.A., J.L-S., K.C.; Data Visualization: S.H., J.L-S., K.C; Supervision: J.L-S., K.C; Project Administration & Funding acquisition: K.A.& K.C.

Financial/non-financial disclosures: Dr. Amrein reports receiving lecture fees from Fresenius Kabi. Drs. Hossain, Lasky-Su, and Christopher report no financial or other relationships that might lead to a conflict of interest

Funding: This work was supported by the National Institutes of Health [R01 GM115774]. The European Society supported the VITdAL-ICU trial for Clinical Nutrition and Metabolism (ESPEN), a research grant including the provision of study medication from Fresenius Kabi (Germany), and the Austrian National Bank (Jubiläumsfonds, Project Nr. 14143).

Running Head: The Metabolomics of Elevated Serum Glucose in Critical Illness

Total word count: 2789

ABSTRACT

Background: In critically ill patients, hyperglycemia is common. Plasma metabolite profiles in critically ill patients allow for a point-in-time picture of the metabolic response to cell stressors. However, the role of the metabolic response to hyperglycemia in the critically ill is still unknown.

Objective: To study the association between serum glucose and plasma metabolites over the first week of critical illness.

Methods: We performed a post-hoc metabolomics analysis of the double-blind, placebo-controlled VITdAL-ICU trial. We analyzed 983 metabolites from a total of 1124 plasma samples from 391 subjects at randomization (day 0), day 3, and 7. Glucose level above and below 150 mg/dl was assigned as the referent as a cut-off value to trigger intervention for hyperglycaemia. The relationships between metabolites and glucose levels were assessed via Student's t-test, orthogonal partial least square-discriminant analysis, and linear mixed-effects models. For repeated measures, data (day 0, 3, and 7), the association between individual metabolites (outcome) over time, and glucose levels from baseline day 0 to day 3 were determined by correcting for age, sex, baseline 25(OH)D, Simplified Acute Physiology Score (SAPS) II, admission diagnosis category, history of diabetes and plasma day (as the random-intercept).

Results: The mean (SD) glucose level at day 0 was 150.3 (51.4) mg/dL. The overall 180-day mortality of the 391 subjects of the analytic cohort was 36.6%. In the mixed-effects modeling, 88 metabolites were found to have significant positive associations with higher glucose levels, where 5 branched-chain amino acids (BCAAs

) metabolites, 12 diacylglycerols (DAG), and 19 glycerophospholipids, specifically phosphatidylcholine (PC), phosphatidylethanolamine (PE), and phosphatidylinositol (PI), and Triacylglycerols (TAGs) were highlighted.

Conclusion: In critically ill hyperglycemic patients, energy utilization is altered, indicating a metabolic shift involving mitochondria and the endoplasmic reticulum specifically.

Word count: 283

Keywords: critical illness, hyperglycemia, metabolomics, branched-chain amino acid (BCAA), diacylglycerols (DAG), Triacylglycerols (TAGs)

List of non-standard abbreviations: VITdAL-ICU trial- Correction of Vitamin D Deficiency in Critically Ill Patients trial; OPLS-DA- Orthogonal partial least square-discriminant analysis; CV- ANOVA- Cross-validation analysis of variance; SAPS- Simplified Acute Physiology Score

INTRODUCTION

Hyperglycemia is common in critically ill patients and is associated with increased morbidity and mortality (1). Up to 50% of critically ill patients develop hyperglycemia within 48 hours of ICU admission (2). Hyperglycemia develops via increased gluconeogenesis, accelerated glycogenolysis, and impaired glucose utilization by peripheral tissues during critical illness (3). In critically ill patients, metabolic stress causes glycogen breakdown, catecholamine and adrenocorticotrophic hormone synthesis, glucagon synthesis, and insulin resistance in the pro-inflammatory phase, all contributing to hyperglycemia (4). Critically ill patients with blood glucose>180 mg/dl in the presence of acute illness without previously diagnosed diabetes have significantly higher mortality compared to patients with previously confirmed diabetes or normoglycemia (5).

Hyperglycemia in critical illness results from hepatic gluconeogenesis and glycogen breakdown due to catecholamine release and direct sympathetic stimulation, respectively (6, 7). Glucose metabolism is influenced directly by cytokines and indirectly via classical glucoregulatory hormone stimulation (8). Hyperglycemia is promoted by inhibiting insulin release in a concentration-dependent manner by TNF, IFNα, GM-CSF, and IL-6 (9-11). In addition, insulin is reported to blunt inflammatory responses in experimental endotoxemia in animal models (12, 13).

Metabolites drive biological processes such as energy generation and storage, signal transduction, and apoptosis. In addition, metabolites are sensitive to cell stress and respond quickly to measurable changes in the blood (14). Metabolomics identifies and quantifies metabolites, metabolic substrates, and cellular products in biofluids, cells, and tissues (15).

Metabolomic studies performed early in critical illness reflect illness severity and predict outcomes (16-18). However, no existent study has defined the metabolic response to hyperglycemia in the critically ill. Therefore, we studied the association between serum glucose and plasma metabolites over the first week of critical illness. We hypothesized that hyperglycemia is associated with metabolism differences related to innate immunity in critically ill patients. We performed a post-hoc metabolomics cohort study of plasma samples from the single center VITdAL-ICU trial, which included 492 critically ill adults with 25-hydroxyvitamin D [25(OH)D] levels ≤ 20 ng/mL randomized to high-dose oral vitamin D3 or placebo (19). We measured the abundance of 983 metabolites from 1124 plasma samples over three-time points (days 0, 3, and 7) in 391 VITdAL-ICU trial subjects (19). We determined the association of increased serum glucose on changes in individual metabolites and metabolic pathways over the first seven days following trial enrollment.

METHODS

During the VITdAL-ICU trial, plasma was collected from 428 subjects (19, 20). Subjects without serum glucose measured at day 0 or 25(OH)D measured at day 0 or day 3 were excluded (Supplementary Figure 1). In addition, we performed a post-hoc metabolomics cohort study on 391 VITdAL-ICU trial subjects. The VITdAL-ICU trial was a double-blind, placebo-controlled, single-center trial conducted in 5 medical and surgical intensive care units in southeast Austria. This study enrolled critically ill adult patients with 25(OH)D 20 ng/mL or lower expected to stay ≥ 48 hrs in ICU. The post-hoc study research protocol was approved by the Partners Human Research Committee Institutional Review Board at the Brigham and Women's Hospital. All research followed the Declaration of Helsinki (Protocol # 2015P002766).

The exposure of interest was serum glucose measured at trial day 0 before intervention. Serum glucose was measured at the same time as day 0 plasma sample was collected for metabolomics. Day 0 serum glucose was studied as continuous, in quartiles, and a binary variable categorized above and below day 0 glucose 150 mg/dl (21-23). Clinical trial data utilized included age, sex, race, admission diagnosis category, baseline 25(OH)D, absolute change in 25(OH)D level at day 3 relative to day 0, and the Simplified Acute Physiology Score (SAPS) II (24) at day 0. In addition, serum 25(OH)D levels were measured by chemiluminescence immunoassay. Admission diagnosis category was determined at ICU admission by trial investigators as Neurosurgery, Cardiac surgery, Cardiovascular, Gastrointestinal/liver, Hematologic/Oncology/

Metabolic, Neurologic, Other non-operative, Other operatives, Renal, Respiratory, Sepsis/infectious, Thoracic Surgery, Transplantation, Trauma, and Vascular Surgery.

A total of 1124 plasma samples were collected between May 2010 and March 2012 from VITdAL-ICU trial subjects at days 0, 3, and 7. Fractionated plasma was aliquoted, stored at -80°C, thawed once, and analyzed in 2017 using four ultra-high-performance liquid chromatography/tandem accurate mass spectrometry methods by Metabolon, Inc (NC, USA) (19). The impact of long-term −80 °C storage for years is almost negligible (25). We analyzed 983 known metabolites per plasma sample. The study sample size was determined via MetaboAnalyst 4.0 with a false discovery rate (FDR) corrected alpha of 0.05 using equations for single time point metabolomics data with binary groups categorized above and below day 0 glucose 150 mg/dl (21-23). To achieve 80% power, our study requires a sample of 140 subjects above and 140 subjects below glucose 150 mg/dl (22). Analysis of repeated plasma metabolomics data is known to increase study power (26) substantially.

STATISTICAL ANALYSIS

All data were analyzed in a complete case analysis fashion. For univariate analysis of day 0 data, a Student's t-test was performed to determine if significant metabolite abundance differences exist by glucose level (above and below 150 mg/dL) using MetaboAnalyst 4.0 (23). A false discovery rate (FDR) adjusted p-value (q-value) of 0.05 was used to identify significant differences (27).

Orthogonal Projections to Latent Structures Discriminant Analysis (OPLS-DA) was used to test whether all 983 measured metabolites as a whole can discriminate between patients with day 0 glucose above and below 150 mg/dL. OPLS-DA was performed to relate the X data to the Y response (28, 29). In our study, X was the metabolite at day 0, and Y was the exposure as a binary serum day 0 glucose above and below 150 mg/dL. We assessed the OPLS-DA model quality via the variation of X explained by the model (R2X(cum)), the goodness-of-fit represented by the percentage of the variation of Y explained by the model (R2), and the predictive performance (Q2). Permutation testing validated the OPLS-DA model (30, 31). The percentage of the variation of the dataset predicted by the model (Permuted Q2) was assessed using a cross-validation test (32, 33). Sevenfold cross-validation analysis of variance (CV-ANOVA) was utilized to determine the OPLS-DA model significance (31). Additionally, response permutation testing was performed to validate the OPLS-DA model (30, 31).

Serum glucose levels were divided into quartiles (Q0-Q3) for survival studies. Survival Analysis between day 0 glucose quartile was determined by the Kaplan-Meier survival curve and the log-rank test (34, 35). For single time point data, correlations between serum glucose level (continuous exposure) at day 0 and individual metabolite abundance (outcome) were determined utilizing linear regression models correcting for age, sex, SAPS II, admission diagnosis category, and 25(OH)D at day 0. A q-value of 0.05 was used for all significant associations (27). For repeated measures data in 391 subjects, the association between serum glucose (continuous exposure) and

abundance of individual metabolites (outcome) at day 0, 3, and 7 were determined utilizing mixed effects linear regression adjusted for age, sex, SAPS II, admission diagnosis category, sample day, 25(OH)D at day 0, and change in 25(OH)D from day 0-3 with an individual subject-specific random-intercept. We performed an additional mixed effects regression with the additional adjustment of a diabetes diagnosis. All linear regression models were analyzed using STATA 16.1MP (College Station, TX).

RESULTS

Baseline characteristics of the analytic cohort (N = 391) were balanced between subjects grouped by glucose level for age, sex, SAPS II, sepsis, intubation, ICU type, day 0 creatinine means, and 180-day mortality. Differences existed with respect to diabetic status, day 0 serum glucose, and triglycerides **(Table 1).** The overall 180-day mortality of the 391 subject analytic cohort was 36.6%. Log-rank test for equality of survivor functions found no significant difference when glucose levels were categorized into quartiles (Figure 1). Differences between patients excluded for the absence of serum glucose (N=37) compared to the analytic cohort were limited to C-reactive protein **(Supplemental Table 1).**

T-test results showed significant differences exist for 15 individual metabolites (q-value threshold of 0.05) in subjects with glucose ≥150 mg/dl compared to those with glucose < 150 mg/dl **(Table 2)**. Highlights included significant decreases in 7 acyl choline metabolites. Regarding differences in metabolomic profiles of subjects with glucose <

150 mg/dl or glucose ≥150 mg/dl at day 0, though the multivariable OPLS-DA models had poor predictability (Q2<0.3), the stability and robustness of the OPLS-DA model was shown by the permutation test (Q2 intercept of -0.358) with a negative permutation Q2 intercept indicating model validity. The cross-validation procedure showed that the groups with glucose < 150 mg/dl or glucose ≥150 mg/dl at day 0 were significantly separated (CV-ANOVA P-value <0.001) **(Table 3).**

In the linear regression analysis, there were significant associations at day 0 between the abundance of 154 individual metabolites (q-value<0.05) and increased day 0 glucose (continuous) following adjustment for age, sex, baseline 25(OH)D, SAPS II, admission diagnosis category and baseline 25(OH)D. Metabolites associated with increased glucose at day 0 included elevated diacylglycerol species and BCAA metabolites, as well as plasma glucose, lactate, and alanine and decreased acyl choline species **(Table 4).**

In mixed effects modeling of 1124 total day 0, 3, and 7 plasma samples from the analytic cohort (N=391), 84 metabolites had significantly positive (q-value<0.05) associations with serum glucose dominated by increases in diacylglycerol species, BCAA metabolites, as well as glycerophospholipid species (phosphatidylcholine, phosphatidylethanolamine, and phosphatidylinositol) and including plasma glucose, alanine, and lactate, **(Table 5**). Conversely, four metabolites had significant negative associations with serum glucose, highlighted by decreases in acyl choline. Similar

significant metabolite patterns were observed in mixed effects models with additional adjustments for diabetes diagnosis (Data not shown).

DISCUSSION

Our large post-hoc metabolomics study evaluated temporal changes in the metabolome in the setting of elevated serum glucose. Clinical trial data is an efficient approach to assessing glucose-specific responses, resulting in novel findings. First, we demonstrate differences in the metabolome of individual patients with elevated glucose ≥150 mg/dl compared to those with glucose < 150 mg/dl. Second, using OPLS-DA in our day 0 data, we demonstrate that the metabolome of individual patients with elevated glucose ≥150 mg/dl is significantly different compared to those with glucose < 150 mg/dl. Third, with linear and mixed effects regression, we show that increasing glucose is associated with differential metabolite patterns at day 0 and over time early in critical illness. Importantly, these patterns manifest as robust increases and decrease in groups of metabolites along the same sub-pathways. These analyses demonstrate evidence of glucose-specific metabolism changes in early critical illness.

Our observations of increases in lactate, alanine, and branched-chain amino acids (BCAAs) with elevated serum day 0 glucose are in line with the classical understanding of the metabolic consequences of hyperglycemia. The liver is central to maintaining blood glucose supply for obligate glucose utilizers (e.g., red blood cells & central nervous system) (36). With fasting, the liver produces glucose via the breakdown of

glycogen and gluconeogenesis with increased substrate delivery of lactate, glycerol, and branched-chain amino acids (BCAAs) via the bloodstream (37). Further, glucose is produced in the liver via the alanine cycle derived from muscle proteins (38). During physiological stress, lactate and alanine are the primary substrates for gluconeogenesis in the liver (39).

We find lipid metabolites, including diacylglycerols (DAG) and glycerophospholipids, specifically phosphatidylcholine, phosphatidylethanolamine, and phosphatidylinositol, are increased in patients with hyperglycemia. During critical illness, endogenous lipids are metabolically active (40, 41). Metabolism of excess lipids to toxic lipids leads to mitochondrial dysfunction and apoptosis (42). DAGs are crucial for structural function and signal transduction and are thus tightly regulated (43). Elevations of DAG are essential for the production and activation of signaling molecules, including cytokines and inflammatory mediators (44, 45). In addition, DAG modulates immune function concerning immunological synapse function and respiratory burst (46, 47). DAG is the substrate for Diacylglycerol kinase α (DGKα), an immune checkpoint to the innate immune system (48). DAG synthesis is shown to be increased with chronic hyperglycemia via the reduction of dihydroxyacetone phosphate to glycerol-3-phosphate but has not been demonstrated in elevated glucose in the critical illness population (49). Changes in DAG with increasing glucose may be related to altered innate immune function.

Glycerophospholipids are glycerol-based phospholipids with phosphate groups modified with choline (phosphatidylcholine), ethanolamine (phosphatidylethanolamine), or inositol (phosphatidylinositol). Glycerophospholipids are the most abundant in mammalian cell membranes and are required for cell survival (50). Glycerophospholipids are essential for regulating insulin secretion in pancreatic cells, mediating insulin activity on skeletal muscle and adipocytes, modulation glucose uptake linked genes, and function of mitochondria as well as energy metabolism (51). Phosphatidylcholine is the major phospholipid found in the blood as a component of lipoproteins (50). Phosphatidylethanolamines are required for autophagy and ferroptosis and enhance oxidative phosphorylation (45, 52-56). Our results underscore the importance of insulin signaling and energy metabolism via glycerophospholipid production in increased circulating glucose.

Our present study approach has multiple strengths. First, repeated measures of plasma samples in individual patients lower intra-patient variability and increase the statistical power of our study (18, 57-59). We used linear mixed–effect models, which are extremely useful for metabolomic data measured at multiple time points and multiple clinical variables early in critical illness as they remove confounding variables with a fixed effect (age, SAPS II, etc.) and also those with a random effect (plasma sampling day) (60, 61). Importantly, by adjusting for the absolute change in 25(OH)D level at day 0,3 and 7, we mitigate the effect of the trial intervention on the observed metabolomic changes associated with hyperglycemia, which allow for the study of the entire trial cohort, increasing the sample size and study power (62, 63). Finally, we used the false

discovery rate adjusted p-value (q-value) threshold of 0.05 to determine all significant differences (27).

Potential limitations exist in our study. First, our cohort may not be generalizable to all critically ill patients as the subjects were recruited from a single large academic medical center. Though our data was generated from a randomized trial, we could not exclude the effect of unknown confounders despite multivariable adjustment because of nonrandomized comparisons of metabolite abundance. Despite adjustment for biological sex, the results may be driven by unmeasured confounders related to differences between men and women (64). Additionally, we cannot study racial disparities in metabolomics as the subjects studied were all White (65). Subject data is absent for HbA1C, parenteral nutrition, dextrose use, and dose and duration of medications that can contribute to elevated glucose. Although significant differences in plasma metabolites with documented biological and functional significance were identified, it may not be clear what a change in metabolite abundance means clinically. Lastly, as our study is post-hoc, our inferences require external validation and should be considered hypothesis-generating.

CONCLUSIONS

Our data suggest that in critically ill hyperglycemic patients, a classical response is present with increased lactate, alanine, and branched-chain amino acids (BCAAs) metabolites but also increases in diacylglycerol and glycerophospholipids species. Further understanding of how alterations in metabolite response to elevated glucose

regulate immunity, insulin signaling, and energy metabolism could provide novel therapies for the dysregulation of metabolic homeostasis in critical illness.

Figure Legends

Figure 1. Kaplan–Meier Estimates of Survival. Kaplan–Meier estimates overall survival by serum glucose quartiles at day 0 (N=391). The log-rank test revealed a significant difference in survival between the quartiles (P=0.5).

Figure 2. OPLS-DA score Plot. t1: The predicted principal components-score value of main components and the difference between day 0 Glucose <150 mg/dL and day 0 Glucose ≥150 mg/dL, t01: Orthogonal principal component-score value of orthogonal components and difference in the observation group. Blue circles represent the metabolome of individual subjects at day 0 with day 0 Glucose <150 mg/dL; Green circles represent the metabolome of individual subjects at day 0 with day 0 Glucose ≥150 mg/dL.

Table 1. Analytic cohort characteristics by Day 0 glucose levels

Baseline Characteristics	**Total**	**Day 0 Glucose <150 mg/dL**	**Day 0 Glucose ≥150 mg/dL**	***P*-value**
No.	391	236	155	
Age Mean (SD)	64.2 (14.8)	63.4 (15.9)	65.4 (13.1)	0.19*
Female No. (%)	138 (35)	75 (54)	63 (46)	0.07
Non-White No. (%)	0 (0)	0 (0)	0 (0)	
Diabetes History No. (%)	96 (25)	45 (19)	41 (33)	0.002
SAPS II Mean (SD)	33.0 (15.6)	33.5 (16.5)	32.1 (14.2)	0.37*
Sepsis No. (%)	28 (7)	17 (7)	11 (7)	0.97
Intubation No. (%)	261 (67)	165 (70)	96 (62)	0.10
ICU				0.61
Anesthesia ICU No. (%)	73 (19)	50 (21)	23 (14)	
Cardiac Surgery ICU No. (%)	116 (30)	66 (28)	50 (32)	
Surgical ICU No. (%)	22 (6)	13 (6)	9 (6)	
Medical ICU No. (%)	81 (21)	48 (20)	33 (21)	
Neurological ICU No. (%)	99 (25)	59 (25)	40 (26)	
Day 0 Glucose Mean (SD)	150.3 (51.4)	120.1 (19.1)	196.1 (51.4)	**<0.001***
Day 0 Creatinine Mean (SD)	1.41 (1.00)	1.37 (0.99)	1.47 (1.02)	0.31*
Triglycerides Mean (SD)	143.2 (95.3)	134.0 (84.1)	157.3 (109.2)	**0.019***
Day 0 C-reactive protein Mean (SD)	121.8 (87.0)	115.9 (79.7)	130.9 (96.6)	0.096*
180-day mortality No. (%)	143 (36.6)	91 (38.6)	52 (33.5)	0.31

Footnote: Data presented as No. (%) unless otherwise indicated. P-values determined by chi-square unless designated by (*), then P-value determined by ANOVA

Table 2. Crude Metabolite abundance differences in patients with day 0 glucose above and below 150 mg/dL

Metabolite	Pathway	t statistic	*P*-value	q-value
3-hydroxybutyrate	BCAA Metabolism	4.9772	9.71E-07	1.06E-04
1,2,3-benzenetriol sulfate	Chemical	3.4741	5.70E-04	3.72E-02
prolyl glycine	Dipeptide	3.8174	1.57E-04	1.28E-02
Dihomo-linolenoyl-choline	Fatty Acid Metabolism (Acyl Choline)	-6.0226	3.98E-09	1.37E-06
Linoleoylcholine	Fatty Acid Metabolism (Acyl Choline)	-5.9612	5.62E-09	1.37E-06
Palmitoylcholine	Fatty Acid Metabolism (Acyl Choline)	-5.9927	4.71E-09	1.37E-06
Arachidonoylcholine	Fatty Acid Metabolism (Acyl Choline)	-5.8881	8.45E-09	1.54E-06
Oleoylcholine	Fatty Acid Metabolism (Acyl Choline)	-5.8685	9.42E-09	1.54E-06
Docosahexaenoylcholine	Fatty Acid Metabolism (Acyl Choline)	-5.0262	7.65E-07	9.35E-05
Stearoylcholine	Fatty Acid Metabolism (Acyl Choline)	-4.9509	1.10E-06	1.08E-04
Fructose	Fructose Metabolism	5.421	1.04E-07	1.46E-05
Glucose	Glycolysis Metabolism	7.5351	3.46E-13	3.38E-10
1-palmitoyl-GPI (16:0)	Lysophospholipid	-3.7792	1.82E-04	1.37E-02
Dihomolinolenate (20:3n3 or 3n6)	Polyunsaturated Fatty Acids (n3 and n6)	-3.5046	5.11E-04	3.57E-02
4-hydroxyphenylpyruvate	Tyrosine Metabolism	3.834	1.47E-04	1.28E-02

Table 3. Day 0 OPLS-DA model goodness of fit, predictive ability, and model significance

	OPLS-DA			Permutation (*n* = 200)		CV-ANOVA
Classification Model	R2X	R2Y	Q2	R2 intercept (*x*-axis, *y*-axis)	Q2 intercept (*x*-axis, *y*-axis)	P-Value
Glucose<150 VS ≥ 150 mg/dl	0.237	1.00	0.242	0.00, 0.448	0.00, -0.358	<0.001

Table 4. Metabolites significantly Increased with Increasing Glucose over day 0

Biochemical	Beta	FDR q-value	Super Pathway	Sub Pathway
glucose	0.004825	3.46E-55	Carbohydrate	Glycolysis, Gluconeogenesis, and Pyruvate
lactate	0.001377	9.40E-04	Carbohydrate	Glycolysis, Gluconeogenesis, and Pyruvate
alanine	0.001422	1.64E-03	Amino Acid	Alanine and Aspartate Metabolism
3hydroxybutyratee	0.003078	6.34E-08	Amino Acid	BCAA Metabolism
propionylglycine (C3)	0.00207	1.88E-03	Lipid	BCAA Metabolism
valine	0.001471	1.87E-04	Amino Acid	BCAA Metabolism
3-hydroxy-2-ethyl propionate	0.001425	1.21E-02	Amino Acid	BCAA Metabolism
N-acetylleucine	0.001371	4.49E-02	Amino Acid	BCAA Metabolism
isoleucine	0.00127	2.68E-03	Amino Acid	BCAA Metabolism
leucine	0.001238	2.86E-03	Amino Acid	BCAA Metabolism
3-methyl-2-oxobutyrate	0.00109	1.92E-02	Amino Acid	BCAA Metabolism
4-methyl-2oxo pentanoate	0.001077	4.66E-02	Amino Acid	BCAA Metabolism
3-methyl-2-oxovalerate	0.001061	4.06E-02	Amino Acid	BCAA Metabolism
palmitoyl-arachidonoyl-glycerol (16:0/20:4) [2]*	0.002064	1.88E-03	Lipid	Diacylglycerol
diacylglycerol (14:0/18:1, 16:0/16:1) [2]*	0.001972	7.45E-03	Lipid	Diacylglycerol
diacylglycerol (14:0/18:1, 16:0/16:1) [1]*	0.001868	1.20E-02	Lipid	Diacylglycerol
palmitoyl-palmitoyl-glycerol (16:0/16:0) [2]*	0.001863	1.33E-02	Lipid	Diacylglycerol
stearoyl-arachidonoyl-glycerol (18:0/20:4) [2]*	0.001695	1.69E-02	Lipid	Diacylglycerol
diacylglycerol (16:1/18:2 [2], 16:0/18:3 [1])*	0.001648	1.52E-02	Lipid	Diacylglycerol
palmitoyl-linoleoyl-glycerol (16:0/18:2) [2]*	0.001646	4.31E-03	Lipid	Diacylglycerol
linoleoyl-linolenoyl-glycerol (18:2/18:3) [2]*	0.001645	2.08E-02	Lipid	Diacylglycerol
palmitoyl-oleoyl-glycerol (16:0/18:1) [2]*	0.00162	8.13E-03	Lipid	Diacylglycerol
linoleoyl-arachidonoyl-glycerol (18:2/20:4) [2]*	0.001607	1.61E-02	Lipid	Diacylglycerol
oleoyl-oleoyl-glycerol (18:1/18:1) [2]*	0.001566	9.16E-03	Lipid	Diacylglycerol
palmitoyl-linoleoyl-glycerol (16:0/18:2) [1]*	0.001546	1.55E-02	Lipid	Diacylglycerol

oleoyl-linoleoyl-glycerol (18:1/18:2) [2]	0.00153	8.13E-03	Lipid	Diacylglycerol
oleoyl-arachidonoyl-glycerol (18:1/20:4) [2]*	0.001527	1.54E-02	Lipid	Diacylglycerol
palmitoyl-oleoyl-glycerol (16:0/18:1) [1]*	0.001482	1.61E-02	Lipid	Diacylglycerol
oleoyl-oleoyl-glycerol (18:1/18:1) [1]*	0.001454	1.31E-02	Lipid	Diacylglycerol
oleoyl-linoleoyl-glycerol (18:1/18:2) [1]	0.001312	2.60E-02	Lipid	Diacylglycerol
1-myristoyl-2-arachidonoyl-GPC (14:0/20:4)*	0.00249	8.17E-06	Lipid	Phosphatidylcholine
1-linoleoyl-2-linolenoyl-GPC (18:2/18:3)*	0.002145	4.15E-03	Lipid	Phosphatidylcholine
1-myristoyl-2-palmitoyl-GPC (14:0/16:0)	0.002014	3.43E-05	Lipid	Phosphatidylcholine
1-palmitoyl-2-oleoyl-GPC (16:0/18:1)	0.00168	3.11E-08	Lipid	Phosphatidylcholine
1-palmitoyl-2-palmitoleoyl-GPC (16:0/16:1)*	0.001578	1.78E-03	Lipid	Phosphatidylcholine
1-stearoyl-2-oleoyl-GPC (18:0/18:1)	0.001544	1.18E-04	Lipid	Phosphatidylcholine
1-palmitoyl-2-arachidonoyl-GPC (16:0/20:4n6)	0.001478	1.98E-05	Lipid	Phosphatidylcholine
1-stearoyl-2-arachidonoyl-GPC (18:0/20:4)	0.001405	4.74E-05	Lipid	Phosphatidylcholine
1-palmitoleoyl-2-linolenoyl-GPC (16:1/18:3)*	0.001383	4.48E-02	Lipid	Phosphatidylcholine
1-palmitoyl-2-docosahexaenoyl-GPC (16:0/22:6)	0.001371	1.20E-04	Lipid	Phosphatidylcholine
1,2-dipalmitoyl-GPC (16:0/16:0)	0.001251	1.87E-03	Lipid	Phosphatidylcholine
1-stearoyl-2-docosahexaenoyl-GPC (18:0/22:6)	0.001239	3.95E-03	Lipid	Phosphatidylcholine
1-palmitoyl-2-linoleoyl-GPC (16:0/18:2)	0.001079	9.75E-04	Lipid	Phosphatidylcholine
1-palmitoyl-2-stearoyl-GPC (16:0/18:0)	0.001042	8.43E-03	Lipid	Phosphatidylcholine
1,2-dipalmitoyl-GPE (16:0/16:0)*	0.002935	6.61E-07	Lipid	Phosphatidylethanolamine
1-stearoyl-2-oleoyl-GPE (18:0/18:1)	0.002254	5.09E-05	Lipid	Phosphatidylethanolamine
1-palmitoyl-2-oleoyl-GPE (16:0/18:1)	0.002207	3.43E-05	Lipid	Phosphatidylethanolamine
1-palmitoyl-2-stearoyl-GPE (16:0/18:0)*	0.00181	2.08E-03	Lipid	Phosphatidylethanolamine
1-stearoyl-2-linoleoyl-GPE (18:0/18:2)*	0.001424	9.70E-03	Lipid	Phosphatidylethanolamine
1-stearoyl-2-arachidonoyl-GPE (18:0/20:4)	0.001317	8.82E-03	Lipid	Phosphatidylethanolamine
1-stearoyl-2-arachidonoyl-GPI (18:0/20:4)	0.001908	2.13E-05	Lipid	Phosphatidylinositol
1-palmitoyl-2-oleoyl-GPI (16:0/18:1)*	0.001853	1.88E-03	Lipid	Phosphatidylinositol
1-stearoyl-2-oleoyl-GPI (18:0/18:1)*	0.001809	5.23E-03	Lipid	Phosphatidylinositol

1-stearoyl-2-linoleoyl-GPI (18:0/18:2)	0.001668	1.04E-03	Lipid	Phosphatidylinositol
1-palmitoyl-2-arachidonoyl-GPI (16:0/20:4)*	0.001394	1.43E-02	Lipid	Phosphatidylinositol

Note: Significant results were presented following individual mixed effects modeling of each of the 983 individual metabolites measured at day 0. All estimates were adjusted for age, sex, SAPS II, admission diagnosis, and 25(OH)D at randomization. A multiple test-corrected thresholds of $q < 0.05$ was used to identify all significant associations. GPC is Glycerophosphorylcholine; GPE is glycerophosphoethanolamine. Positive β coefficient values indicate higher metabolite abundance with increasing day 0 serum glucose.

Table 5. Metabolites significantly Increased with Increasing Glucose over days 0, 3 and 7

Biochemical	Beta	FDR q-value	Super Pathway	Sub Pathway
Glucose	0.002397374	3.38E-42	Carbohydrate	Glycolysis, Gluconeogenesis, and Pyruvate
Alanine	0.000847026	2.45E-02	Amino Acid	Alanine and Aspartate Metabolism
Lactate	0.000769368	4.32E-02	Carbohydrate	Glycolysis, Gluconeogenesis, and Pyruvate
3-hydroxybutyrate	0.001861057	1.01E-05	Amino Acid	BCAA Metabolism
propionylglycine (C3)	0.00137764	1.01E-02	Lipid	BCAA Metabolism
Valine	0.000834214	8.86E-03	Amino Acid	BCAA Metabolism
Leucine	0.00083406	1.05E-02	Amino Acid	BCAA Metabolism
Isoleucine	0.000643604	4.32E-02	Amino Acid	BCAA Metabolism
palmitoyl-arachidonoyl-glycerol (16:0/20:4) [2]*	0.001896931	3.08E-04	Lipid	Diacylglycerol
palmitoyl-arachidonoyl-glycerol (16:0/20:4) [1]*	0.001696208	3.31E-03	Lipid	Diacylglycerol
oleoyl-arachidonoyl-glycerol (18:1/20:4) [2]*	0.001533007	3.31E-03	Lipid	Diacylglycerol
palmitoyl-palmitoyl-glycerol (16:0/16:0) [2]*	0.00150837	1.43E-02	Lipid	Diacylglycerol
linoleoyl-arachidonoyl-glycerol (18:2/20:4) [2]*	0.001435998	7.85E-03	Lipid	Diacylglycerol
diacylglycerol (14:0/18:1, 16:0/16:1) [2]*	0.001410765	1.73E-02	Lipid	Diacylglycerol
diacylglycerol (14:0/18:1, 16:0/16:1) [1]*	0.00138089	1.83E-02	Lipid	Diacylglycerol
palmitoyl-oleoyl-glycerol (16:0/18:1) [2]*	0.001286221	1.09E-02	Lipid	Diacylglycerol
oleoyl-arachidonoyl-glycerol (18:1/20:4) [1]*	0.001258482	1.50E-02	Lipid	Diacylglycerol
palmitoyl-oleoyl-glycerol (16:0/18:1) [1]*	0.00120317	1.81E-02	Lipid	Diacylglycerol
oleoyl-oleoyl-glycerol (18:1/18:1) [2]*	0.001048803	4.32E-02	Lipid	Diacylglycerol
1-myristoyl-2-arachidonoyl-GPC (14:0/20:4)*	0.002022287	2.35E-05	Lipid	Phosphatidylcholine
1-linoleoyl-2-linolenoyl-GPC (18:2/18:3)*	0.001471315	9.67E-03	Lipid	Phosphatidylcholine
1-myristoyl-2-palmitoyl-GPC (14:0/16:0)	0.001435581	2.99E-03	Lipid	Phosphatidylcholine

1-palmitoyl-2-palmitoleoyl-GPC (16:0/16:1)*	0.001171801	2.11E-02	Lipid	Phosphatidylcholine
1-palmitoyl-2-oleoyl-GPC (16:0/18:1)	0.001158139	1.49E-05	Lipid	Phosphatidylcholine
1-stearoyl-2-oleoyl-GPC (18:0/18:1)	0.001149058	1.76E-03	Lipid	Phosphatidylcholine
1-palmitoyl-2-docosahexaenoyl-GPC (16:0/22:6)	0.000982429	5.59E-03	Lipid	Phosphatidylcholine
1-stearoyl-2-docosahexaenoyl-GPC (18:0/22:6)	0.000952075	2.78E-02	Lipid	Phosphatidylcholine
1-palmitoyl-2-arachidonoyl-GPC (16:0/20:4n6)	0.000925918	5.35E-03	Lipid	Phosphatidylcholine
1-stearoyl-2-arachidonoyl-GPC (18:0/20:4)	0.000863441	9.55E-03	Lipid	Phosphatidylcholine
1,2-dipalmitoyl-GPE (16:0/16:0)*	0.00193856	2.35E-05	Lipid	Phosphatidylethanolamine
1-palmitoyl-2-oleoyl-GPE (16:0/18:1)	0.001598293	2.99E-03	Lipid	Phosphatidylethanolamine
1-stearoyl-2-oleoyl-GPE (18:0/18:1)	0.001584726	6.96E-03	Lipid	Phosphatidylethanolamine
1-palmitoyl-2-stearoyl-GPE (16:0/18:0)*	0.001370249	1.01E-02	Lipid	Phosphatidylethanolamine
1-palmitoyl-2-oleoyl-GPI (16:0/18:1)*	0.001499492	2.99E-03	Lipid	Phosphatidylinositol
1-stearoyl-2-oleoyl-GPI (18:0/18:1)*	0.001458036	1.01E-02	Lipid	Phosphatidylinositol
1-stearoyl-2-arachidonoyl-GPI (18:0/20:4)	0.001138683	3.48E-03	Lipid	Phosphatidylinositol
1-palmitoyl-2-arachidonoyl-GPI (16:0/20:4)*	0.001129459	1.15E-02	Lipid	Phosphatidylinositol
1-stearoyl-2-linoleoyl-GPI (18:0/18:2)	0.001053291	1.96E-02	Lipid	Phosphatidylinositol

Note: Significant results were presented following individual mixed effects modeling of each of the 983 individual metabolites measured at days 0,3, and 7. All estimates were age, sex, SAPS II, admission diagnosis, 25(OH)D at randomization, absolute change in 25(OH)D level at day 3, plasma day, and individual patient (as the random-intercept). A multiple test-corrected thresholds of $q < 0.05$ was used to identify all significant associations. GPC is Glycerophosphorylcholine; GPE is glycerophosphoethanolamine. Positive β coefficient values indicate higher metabolite abundance with increasing day 0 serum glucose.

Figure 1. Survival analysis for day 0 glucose quartiles (Q0-Q3).

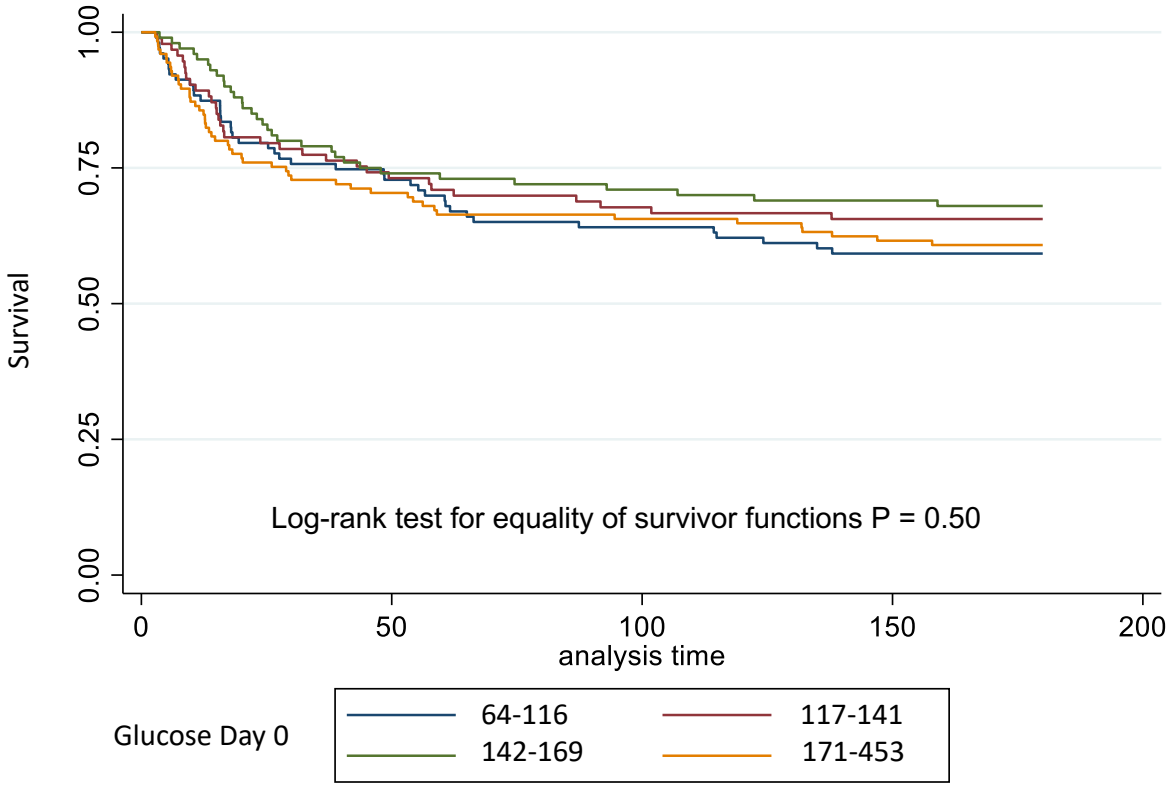

Figure 2. Day 0 OPLS-DA

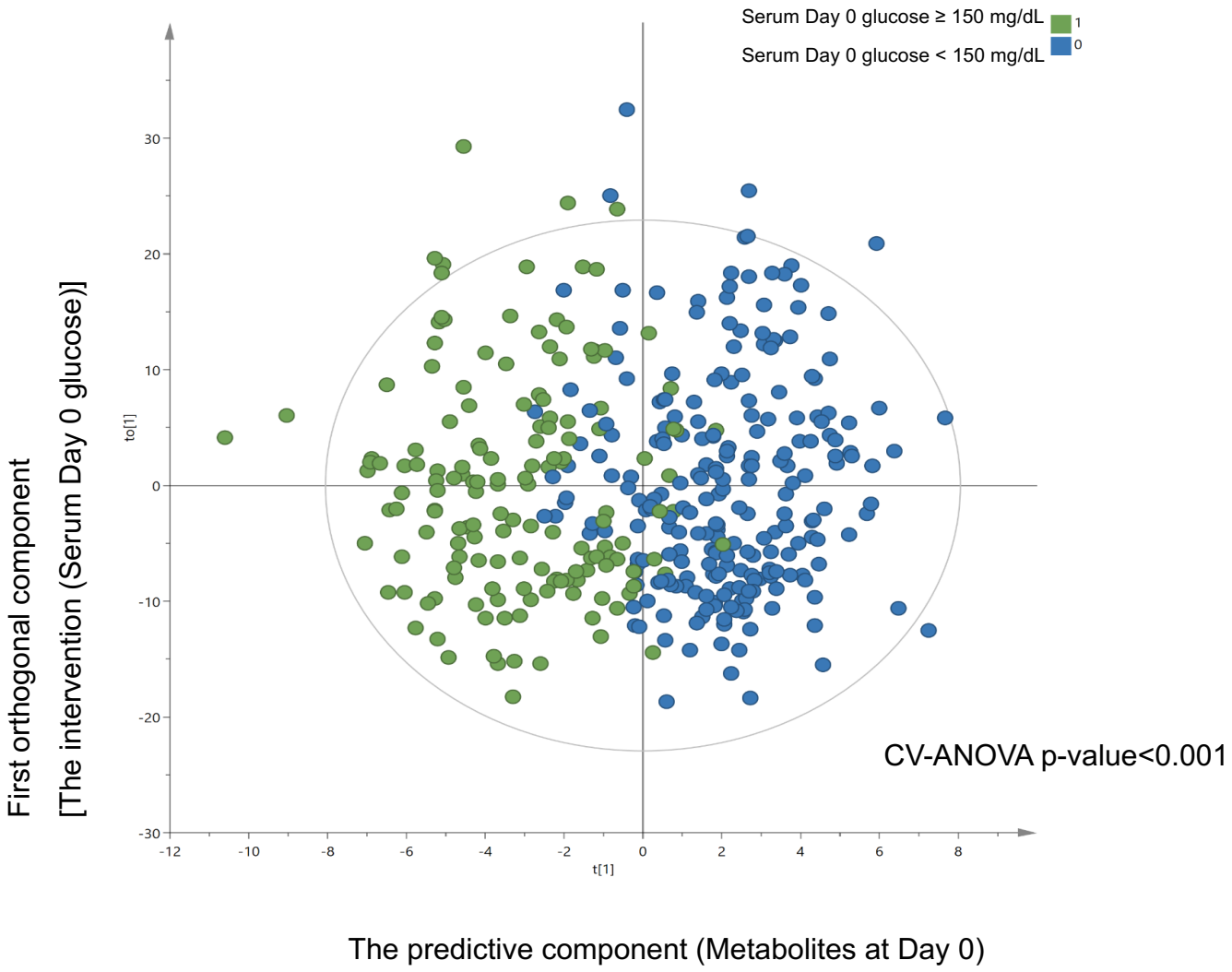

SUPPLEMENTARY METHODS

VITdAL-ICU Cohort Details: The VITdAL-ICU trial randomized 475 critically ill adult subjects with 25(OH)D < 20 ng/mL to vitamin D_3 or placebo given orally or via nasogastric tube once at a dose of 540,000 IU followed by 90,000 IU monthly (1). The trial was conducted at the University Hospital Graz in Southeast Austria in 5 Medical and Surgical Intensive Care Units. Patients were randomized 1:1 with a randomization block size of 8 stratified via ICU type and sex. The primary study outcome was the length of hospital stay. Secondary outcomes included 28-day mortality, hospital mortality, 6-month mortality, length of ICU stay, and 25-hydroxyvitamin D (25(OH)D) levels at day 0, 3, and 7. Blood samples were collected on days 0 (pre-randomization), 3, and 7. Plasma was fractionated, aliquoted, and stored at -70°C. Four hundred fifty-three trial subjects had frozen plasma available for analysis. The VITdAL-ICU trial was approved by the institutional ethical committee of the Medical University of Graz and the Austrian Agency for Health and Food Safety. Following Austrian and European Union requirements and the principles of the Declaration of Helsinki, (2) at VITdAL-ICU trial enrollment, written informed consent was obtained, if possible, directly from the patient or a legal surrogate (1). Consent included permission for plasma specimens to be saved for future research studies. The post-hoc study research protocol was approved by the Mass General Brigham Human Research Committee Institutional Review Board at the Brigham and Women's Hospital (Protocol# 2015P002766).

Clinical trial data utilized included age, sex, admission diagnosis category, baseline 25(OH)D, intervention status (placebo vs. high dose vitamin D_3), absolute change in

25(OH)D level at day 3 relative to day 0, and the Simplified Acute Physiology Score (SAPS) II (3) at day 0. In addition, 25(OH)D levels were measured in the VITdAL-ICU cohort by chemiluminescence immunoassay (1). Admission diagnosis category was determined at ICU admission by trial investigators as Neurosurgery, Cardiac surgery, Cardiovascular, Gastrointestinal/liver, Hematologic/Oncology/ Metabolic, Neurologic, Other non-operative, Other operatives, Renal, Respiratory, Sepsis/infectious, Thoracic Surgery, Transplantation, Trauma, and Vascular Surgery.

Sample Preparation: Blood samples were drawn and transferred into EDTA-coated blood collection tubes within 24 hours from study inclusion and processed within 4 hours after venipuncture. Subsequently, plasma was fractionated, aliquoted, and stored at -80°C [4]. For the VITdAL-ICU subject, 150 µl plasma aliquots were shipped separately on dry ice to Metabolon, Inc at different times. Following receipt, the frozen plasma samples were immediately stored at -80^{o}C. Other investigators note metabolites to be stable for at least two freeze-thaw cycles(5). To generate metabolomic data for the VITdAL-ICU cohort, a total of 1215 VITdAL-ICU trial plasma samples from 428 subjects on day 0, 413 subjects on day 3, and 374 subjects on day seven were prepared and analyzed in 2017(1,6,7).

Plasma sample preparation was performed with the automated MicroLab STAR® Liquid Handling system (Hamilton Company, NV, USA). Before extraction, samples were fortified with quality control (QC) recovery standards. To remove protein, dissociate small molecules bound to protein or trapped in the precipitated protein matrix, and

recover chemically diverse metabolites, proteins were precipitated with methanol via 2 minutes of robust shaking (GenoGrinder 2000 SPEX SamplePrep, NJ, USA) and subsequent centrifugation. The resulting extract was divided into five fractions: two for analysis by two separate reverse phases (RP)/ UPLC-MS/MS methods with positive ion mode electrospray ionization (ESI), one for analysis by RP/UPLC-MS/MS with negative ion mode ESI, one for analysis by HILIC/UPLC-MS/MS with negative ion mode ESI, and one sample was reserved for backup. Samples were placed on a TurboVap® (Zymark, MA, USA) to remove the organic solvent and stored overnight under nitrogen before preparation for analysis.

Quality Assurance (QA) and Quality Control (QC): Several types of controls were utilized with the plasma samples analysis allowing for instrument performance monitoring and aided chromatographic alignment: a pooled matrix sample generated by taking a small volume of each experimental sample served as a technical replicate throughout the data set (8); extracted water samples served as process blanks (9); and a cocktail of QC standards that were carefully chosen not to interfere with the measurement of endogenous compounds were spiked into every analyzed sample(10). Instrument variability was determined by calculating the median relative standard deviation (RSD) for the standards added to each sample before injection into the mass spectrometers(11). Overall process variability was determined by calculating the median RSD for all endogenous metabolites (i.e., non-instrument standards) in 100% of the pooled matrix samples. Experimental samples were randomized across the platform, with QC samples spaced evenly among the injections.

Ultrahigh Performance Liquid Chromatography-Tandem Mass Spectroscopy (UPLC-MS/MS): All methods utilized a Waters ACQUITY ultra-performance liquid chromatography (UPLC) (Waters, MA, USA) and for untargeted lipidomic analysis a Thermo Scientific Q Exactive™ high resolution/accurate mass spectrometer interfaced with a heated electrospray ionization (HESI-II) source and Orbitrap™ mass analyzer operated at 35,000 mass resolution (ThermoFisher Scientific, MA, USA) (12). The sample extract was dried and then reconstituted in solvents compatible with each of the four methods. Each reconstitution solvent contained a series of standards at fixed concentrations to ensure injection and chromatographic consistency. One aliquot was analyzed using acidic positive ion conditions, chromatographically optimized for more hydrophilic compounds. In this method, the extract was gradient eluted from a C18 column (Waters UPLC BEH C18-2.1x100 mm, 1.7 µm) using water and methanol, containing 0.05% perfluoropentanoic acid (PFPA) and 0.1% formic acid (FA). Another aliquot was also analyzed using acidic positive ion conditions; however, it was chromatographically optimized for more hydrophobic compounds(13,14). In this method, the extract was gradient eluted from the same C18 column using methanol, acetonitrile, water, 0.05% PFPA, and 0.01% FA and was operated at an overall higher organic content. Another aliquot was analyzed using basic negative ion optimized conditions using a separate dedicated C18 column. However, the basic extracts were gradient eluted from the column using methanol and water, with 6.5mM Ammonium Bicarbonate at pH 8. The fourth aliquot was analyzed via negative ionization following elution from a HILIC column (Waters UPLC BEH Amide 2.1x150 mm, 1.7 µm) using a gradient

consisting of water and acetonitrile with 10mM Ammonium Formate, pH 10.8. The MS analysis alternated between MS and data-dependent MS^n scans using dynamic exclusion(15). The scan range for both ionization modes was 70–1000 *m/z* (16).

Data Extraction and Compound Identification: Raw data was extracted, peak-identified, and QC processed using Metabolon's hardware and software. Compounds were identified compared to library entries of purified standards or recurrent unknown entities. Metabolon maintains a library based on authenticated standards that contain the retention time/index (RI), the mass-to-charge ratio (*m/z*), and chromatographic data (including MS/MS spectral data) on all molecules present in the library. Furthermore, biochemical identifications are based on three criteria: retention index within a narrow RI window of the proposed identification, accurate mass match to the library +/- 10 ppm, and the MS/MS forward and reverse scores between the experimental data and authentic standards (17). The MS/MS scores are based on comparing the ions present in the experimental spectrum to those in the library spectrum. While there may be similarities between these molecules based on one of these factors, all three data points can be used to distinguish and differentiate biochemicals(18). More than 3300 commercially available purified standard compounds have been acquired and registered into the Metabolon Laboratory Information Management System (LIMS) system for analysis on all platforms to determine their analytical characteristics. The identification level reported in our tables follows the criteria described by Sumner et al. (19). Level 1 is a validated identification that confirms a structure with a minimum of two independent and orthogonal data from a pure reference standard under identical analytical

conditions. Predictive or externally acquired structure evidence when a reference standard does not exist (i.e., MS/MS data exhibiting diagnostic fragments or neutral losses consistent with a specific structure) is a putative identification (Level 2) (20). Compounds labeled with "*" have identification Level 2. If no label is applied, the identification Level is 1. Compounds labeled with "( )" or "[ ]" indicate a structural isomer of another compound in the spectral library; for example, a steroid that may be sulfated at one of several positions that are indistinguishable by the mass spectrometry data or a diacylglycerol for which more than one stereospecific molecule exists. For the Acylcarnitine sub pathway: a capital C is followed by the number of carbons within the fatty acyl group attached to the carnitine. A colon followed by a number is one or more unsaturated carbons in the acylcarnitine ester (i.e., C10:1 is a monounsaturated C10 acylcarnitine). DC following the carbon number is a dicarboxylic acylcarnitine. Acylcarnitines are classified by the number of carbon atoms in the acyl group chain: short-chain acylcarnitines C2 to C7; medium-chain acylcarnitines C8 to C14; long-chain acylcarnitines C16 – C26 (21). A summary of all 983 metabolites identified is present in Supplementary Data 2.

Curation: Various curation procedures were carried out to ensure a high-quality data set was available for statistical analysis and interpretation. The QC and curation processes were designed to ensure accurate and consistent identification of true chemical entities and to remove those representing system artifacts, mis-assignments, and background noise. Metabolon data analysts use proprietary visualization and interpretation software to confirm the consistency of peak identification among the

various samples. Library matches for each compound were checked for each sample and corrected if necessary.

Metabolite Quantification and Data Normalization: Peaks were quantified using total spectral area (area under the curve) (21-23). Metabolite quantitation or abundance is defined as the total ion count for the given mass-to-charge ratio (*m/z*) assigned to the particular metabolite(24). Specifically, metabolite quantitation is determined using extracted ion chromatograms by focusing the narrow mass window on the theoretical *m/z* value of the individual metabolite of interest and eliminating overlapping isobaric signals with the maintenance of mass accuracy during the acquisition(25-29). In addition, a data normalization step was performed to correct variation resulting from instrument inter-day tuning differences. Each compound was corrected in run-day blocks by registering the medians to equal one (1.00) and normalizing each data point proportionately.

Statistical Analysis: Determination of the changes in relative concentrations of metabolites was first suggested as a strategy to define the metabolome in 1998 (30). We analyzed 983 known metabolites per plasma sample. Metabolomic profiling identified 983 metabolites. Metabolomic data underwent a cube root transformation followed by Pareto scaling to generate data on the same scale and followed an approximately normal distribution(31,32).

The study sample size was determined via MetaboAnalyst 4.0 with a false discovery rate (FDR) corrected alpha of 0.05 using equations for single time point metabolomics data with binary groups categorized above and below day 0 glucose 150 mg/dl as ≥ 150 mg/dL (33-35). Glucose level above and below 150 mg/dl was assigned as the referent as a cut-off value to trigger intervention for hyperglycaemia as recommended by the Society of Critical Care Medicine (33). To achieve 80% power, our study requires a sample of 140 subjects above and 140 subjects below glucose 150 mg/dl (34). Analysis of repeated plasma metabolomics data is known to increase study power (36) substantially.

For univariate analysis of day 0 data, a Student's t-test was performed to determine if significant metabolite abundance differences exist by glucose level (above and below 150 mg/dL) using MetaboAnalyst 4.0 (35). A false discovery rate (FDR) adjusted p-value (q-value) of 0.05 was used to identify significant differences (37). Orthogonal Projections to Latent Structures Discriminant Analysis (OPLS-DA) was used to test whether all 983 measured metabolites as a whole can discriminate between patients with day 0 glucose above and below 150 mg/dL. OPLS-DA was performed to relate the X data to the Y response (38,39). In our study, X was the metabolite at day 0, and Y was the exposure as a binary serum day 0 glucose above and below 150 mg/dL. We assessed the OPLS-DA model quality via the variation of X explained by the model (R2X(cum)), the goodness-of-fit represented by the percentage of the variation of Y explained by the model (R2), and the predictive performance (Q2). Permutation testing was performed to validate the OPLS-DA model (40,41). The percentage of the variation of the dataset predicted by the model (Permuted Q2) was assessed using a cross-

validation test (42,43). Sevenfold cross-validation analysis of variance (CV-ANOVA) was utilized to determine the OPLS-DA model significance (41). Additionally, response permutation testing was performed to validate the OPLS-DA model (40,41).

Serum glucose levels were divided into quartiles (Q0-Q3) for survival studies. The survival analysis between the day 0 glucose quartile was determined by the Kaplan-Meier survival curve and the log-rank test (44,45). For single time point data, correlations between serum glucose level (continuous exposure) at day 0 and individual metabolite abundance (outcome) were determined utilizing linear regression models correcting for age, sex, SAPS II, admission diagnosis category, and 25(OH)D at day 0. A q-value of 0.05 was used for all significant associations (37). For repeated measures data in 391 subjects, the association between serum glucose (continuous exposure) and abundance of individual metabolites (outcome) at day 0, 3, and 7 were determined utilizing mixed effects linear regression adjusted for age, sex, SAPS II, admission diagnosis category, sample day, 25(OH)D at day 0, and change in 25(OH)D from day 0-3 with an individual subject-specific random-intercept. In addition, we performed an additional mixed effects regression with the additional adjustment of a diabetes diagnosis. All linear regression models were analyzed using STATA 16.1MP (College Station, TX).

Supplemental Table 1. Characteristics of Subjects excluded for lack of serum Glucose on day 0

Baseline Characteristics	Day 0 Serum Glucose absent	Day 0 Serum Glucose Present	Total	*P*-value
No.	37	391	428	
Age Mean (SD)	63.4 (15.7)	64.2 (14.8)	64.2 (14.9)	**0.75***
Female No. (%)	13 (35.14)	138 (35.29)	151 (35.28)	0.99
Non-White No. (%)	0 (0)	0 (0)	0 (0)	
Diabetes History No. (%)	5 (13.51)	96 (24.55)	101 (23.6)	0.13
SAPS II Mean (SD)	37.7 (12.3)	33 (15.6)	33.4 (15.4)	0.073*
Sepsis No. (%)	3 (8.11)	28 (7.16)	31 (7.24)	0.83
Intubation No. (%)	18 (48.64)	261 (66.75)	279 (65.19)	0.45
ICU				0.48
Anesthesia ICU No. (%)	10 (27.03)	73 (18.67)	81 (19.24)	
Cardiac Surgery ICU No. (%)	8 (21.62)	116 (29.67)	123 (29.22)	
Medical ICU No. (%)	10 (27.03)	81 (20.72)	89 (21.14)	
Neurological ICU No. (%)	8 (21.62)	99 (25.32)	106 (25.18)	
Surgical ICU No. (%)	1 (2.70)	22 (5.63)	22 (5.23)	
Day 0 Creatinine Mean (SD)	1.3 (0.9)	1.4 (1.0)	1.4 (1.0)	**0.54***
Triglycerides Mean (SD)	158.5 (115.2)	143.2 (95.3)	144.3 (96.8)	**0.40***
Day 0 C-reactive protein Mean (SD)	158.6 (113.0)	121.8 (87.0)	124.9 (89.8)	**0.02***
180-day mortality No. (%)	12 (32.43)	143 (36.57)	155 (36.21)	0.62

Supplemental Figure 1. Consort flow diagram

Manuscript # 1

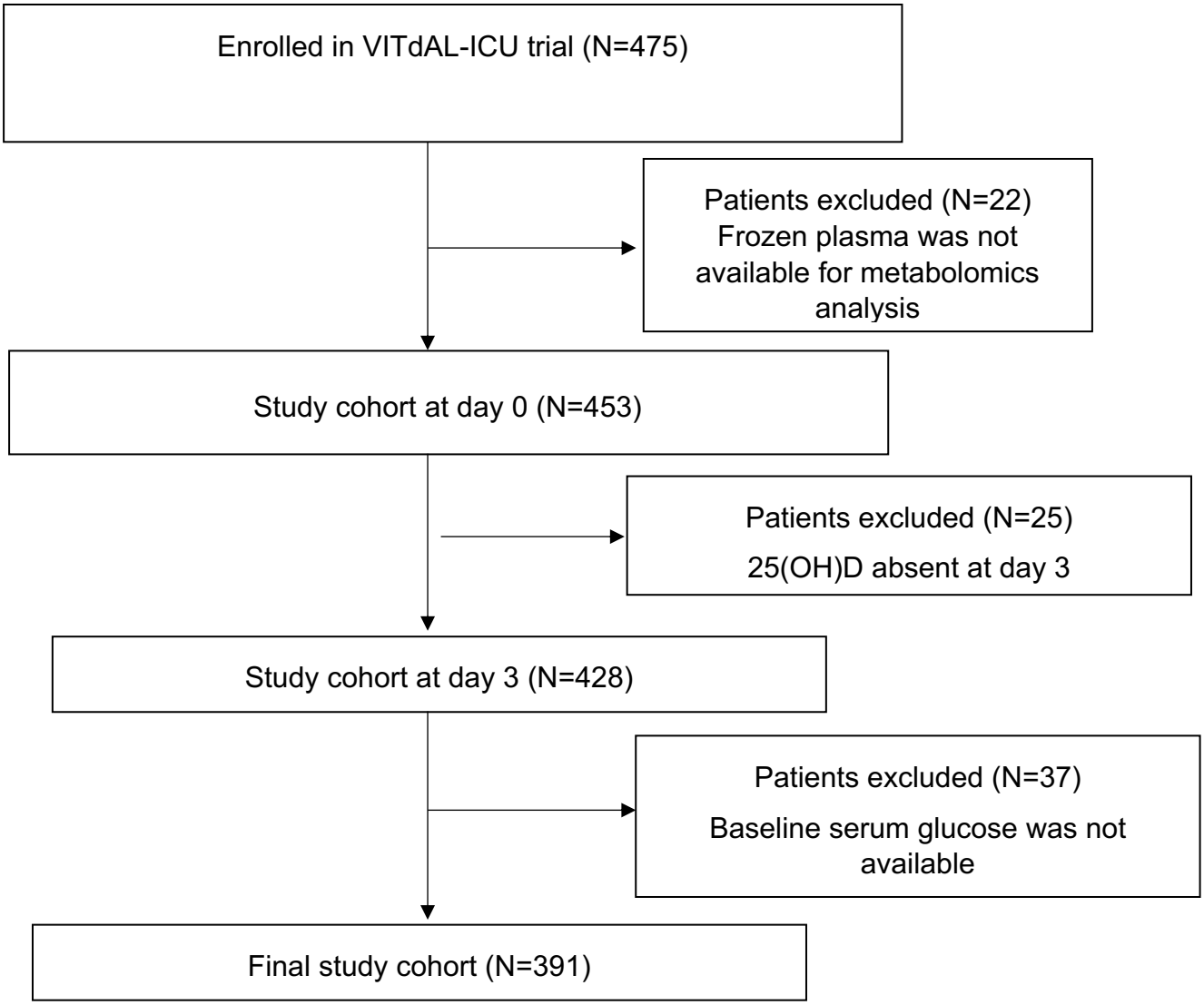

SUPPLEMENTARY METHODS REFERENCES CITED

1. Amrein K, Schnedl C, Holl A, Riedl R, Christopher KB, Pachler C, Urbanic Purkart T, Waltensdorfer A, Munch A, Warnkross H, et al.: Effect of high-dose vitamin D3 on hospital length of stay in critically ill patients with vitamin D deficiency: the VITdAL-ICU randomized clinical trial. JAMA 2014, 312(15):1520-1530.

2. World Medical A: World Medical Association Declaration of Helsinki: ethical principles for medical research involving human subjects. JAMA 2013, 310(20):2191-2194.

3. Le Gall JR, Lemeshow S, Saulnier F: A new Simplified Acute Physiology Score (SAPS II) based on a European/North American multicenter study. JAMA 1993, 270(24):2957-2963.

4. Dolinay T, Kim YS, Howrylak J, Hunninghake GM, An CH, Fredenburgh L, Massaro AF, Rogers A, Gazourian L, Nakahira K et al.: Inflammasome-regulated cytokines are critical mediators of acute lung injury. Am J Respir Crit Care Med 2012, 185(11):1225-1234.

5. Breier M, Wahl S, Prehn C, Fugmann M, Ferrari U, Weise M, Banning F, Seissler J, Grallert H, Adamski J, et al.: Targeted metabolomics identifies reliable and stable metabolites in human serum and plasma samples. PLoS One 2014, 9(2):e89728.

6. Chary S, Amrein K, Lasky-Su J, Dobnig H, Christopher KB: The Sex-specific Metabolic Response to Critical Illness: a post-hoc metabolomics study of the VITdAL-ICU trial. Scientific Reports 2021, 11:3951.

7. Amrein K, Lasky-Su JA, Dobnig H, Christopher KB: Metabolomic basis for response to high dose vitamin D in critical illness. Clinical nutrition 2020.

8. Wehrens R, Hageman JA, van Eeuwijk F, Kooke R, Flood PJ, Wijnker E, Keurentjes JJ, Lommen A, van Eekelen HD, Hall RD et al.: Improved batch correction in untargeted MS-based metabolomics. Metabolomics 2016, 12:88.

9. Trezzi JP, Jager C, Galozzi S, Barkovits K, Marcus K, Mollenhauer B, Hiller K: Metabolic profiling of body fluids and multivariate data analysis. MethodsX 2017, 4:95-103.

10. Bain JR, Stevens RD, Wenner BR, Ilkayeva O, Muoio DM, Newgard CB: Metabolomics applied to diabetes research: moving from information to knowledge. Diabetes 2009, 58(11):2429-2443.

11. Parsons HM, Ekman DR, Collette TW, Viant MR: Spectral relative standard deviation: a practical benchmark in metabolomics. Analyst 2009, 134(3):478-485.

12. Narvaez-Rivas M, Zhang Q: Comprehensive untargeted lipidomic analysis using core-shell C30 particle column and high field orbitrap mass spectrometer. J Chromatogr A 2016, 1440:123-134.

13. Michopoulos F, Lai L, Gika H, Theodoridis G, Wilson I: UPLC-MS-based analysis of human plasma for metabonomics using solvent precipitation or solid phase extraction. J Proteome Res 2009, 8(4):2114-2121.

14. Want EJ, Smith CA, Qin C, Van Horne KC, Siuzdak G: Phospholipid capture combined with non-linear chromatographic correction for improved serum metabolite profiling. Metabolomics 2006, 2:145-154.

15. Oresic M, Vidal-Puig A, Hanninen V: Metabolomic approaches to phenotype characterization and applications to complex diseases. Expert Rev Mol Diagn 2006, 6(4):575-585.

16. Chen WW, Freinkman E, Wang T, Birsoy K, Sabatini DM: Absolute Quantification of Matrix Metabolites Reveals the Dynamics of Mitochondrial Metabolism. Cell 2016, 166(5):1324-1337 e1311.

17. Hufsky F, Scheubert K, Bocker S: Computational mass spectrometry for small-molecule fragmentation. TrAC Trends Anal Chem 2014, 53:41–48.

18. Dunn WB, Broadhurst D, Begley P, Zelena E, Francis-McIntyre S, Anderson N, Brown M, Knowles JD, Halsall A, Haselden JN, et al.: Procedures for large-scale metabolic profiling of serum and plasma using gas chromatography and liquid chromatography coupled to mass spectrometry. Nat Protoc 2011, 6(7):1060-1083.

19. Sumner LW, Amberg A, Barrett D, Beale MH, Beger R, Daykin CA, Fan TW, Fiehn O, Goodacre R, Griffin JL, et al.: Proposed minimum reporting standards for chemical analysis Working Group (CAWG) Metabolomics Standards Initiative (MSI). Metabolomics 2007, 3(3):211-221.

20. Schrimpe-Rutledge AC, Codreanu SG, Sherrod SD, McLean JA: Untargeted Metabolomics Strategies-Challenges and Emerging Directions. J Am Soc Mass Spectrom 2016, 27(12):1897-1905.

21. Weljie AM, Newton J, Mercier P, Carlson E, Slupsky CM: Targeted profiling: quantitative analysis of 1H NMR metabolomics data. Anal Chem 2006, 78(13):4430-4442.

22. Wishart DS: Quantitative metabolomics using NMR. TrAC Trends Anal Chem 2008, 27:228–237.

23. Zhou B, Xiao JF, Tuli L, Ressom HW: LC-MS-based metabolomics. Mol Biosyst 2012, 8(2):470-481.

24. Parisi LR, Li N, Atilla-Gokcumen GE: Very Long Chain Fatty Acids Are Functionally Involved in Necroptosis. Cell Chem Biol 2017, 24(12):1445-1454 e1448.

25. Junot C, Madalinski G, Tabet JC, Ezan E: Fourier transform mass spectrometry for metabolome analysis. Analyst 2010, 135(9):2203-2219.

26. Kamleh A, Barrett MP, Wildridge D, Burchmore RJ, Scheltema RA, Watson DG: Metabolomic profiling using Orbitrap Fourier transform mass spectrometry with hydrophilic interaction chromatography: a method with wide applicability to analysis of biomolecules. Rapid Commun Mass Spectrom 2008, 22(12):1912-1918.

27. Kamleh MA, Hobani Y, Dow JA, Watson DG: Metabolomic profiling of Drosophila using liquid chromatography Fourier transform mass spectrometry. FEBS Lett 2008, 582(19):2916-2922.

28. Koulman A, Woffendin G, Narayana VK, Welchman H, Crone C, Volmer DA: High-resolution extracted ion chromatography, a new tool for metabolomics and lipidomics using a second-generation orbitrap mass spectrometer. Rapid Commun Mass Spectrom 2009, 23(10):1411-1418.

29. Xiao JF, Zhou B, Ressom HW: Metabolite identification and quantitation in LC-MS/MS-based metabolomics. Trends Analyt Chem 2012, 32:1-14.

30. Oliver SG, Winson MK, Kell DB, Baganz F: Systematic functional analysis of the yeast genome. Trends Biotechnol 1998, 16(9):373-378.

31. van den Berg RA, Hoefsloot HC, Westerhuis JA, Smilde AK, van der Werf MJ: Centering, scaling, and transformations: improving the biological information content of metabolomics data. BMC Genomics 2006, 7:142.

32. Struja T, Eckart A, Kutz A, Huber A, Neyer P, Kraenzlin M, Mueller B, Meier C, Bernasconi L, Schuetz P: Metabolomics for Prediction of Relapse in Graves' Disease: Observational Pilot Study. Front Endocrinol (Lausanne) 2018, 9:623.

33. Jacobi J, Bircher N, Krinsley J, Agus M, Braithwaite SS, Deutschman C, et al. Guidelines for the use of an insulin infusion for the management of hyperglycemia in critically ill patients. Crit Care Med. 2012;40(12):3251-76.

34. van Iterson M, t Hoen PA, Pedotti P, Hooiveld GJ, den Dunnen JT, van Ommen GJ, et al. Relative power and sample size analysis on gene expression profiling data. BMC Genomics. 2009;10:439.

35. Chong J, Xia J. Using MetaboAnalyst 4.0 for Metabolomics Data Analysis, Interpretation, and Integration with Other Omics Data. Methods Mol Biol. 2020;2104:337-60.

36. FitzMaurice GM, Laird NM, Ware JH. Applied longitudinal analysis. Hoboken, New Jersey: Wiley; 2011.

37. Benjamini Y, Hochberg Y. Controlling for false discovery rate: a practical and powerful approach to multiple testing. Journal of the Royal Statistical Society Series B (Methodological). 1995;57:289–300.

38. Bylesjö M, Rantalainen M, Cloarec O, Nicholson JK, Holmes E, Trygg J. OPLS discriminant analysis: combining the strengths of PLS-DA and SIMCA classification. Journal of Chemometrics. 2006;20(8-10):341–51.

39. Trygg J, Wold S. Orthogonal projections to latent structures (O-PLS). J Chemometrics. 2002;16:119–28.

40. Westerhuis JA, Hoefsloot HCJ, Smit S, Vis DJ, Smilde AK, van Velzen EJJ, et al. Assessment of PLSDA cross validation. Metabolomics 2008;4(1):81–9.

41. Eriksson L, Trygg J, Wold S. CV-ANOVA for significance testing of PLS and OPLS models. Journal of Chemometrics. 2008;22(11-12):594-600.

41. Eastment H, Krzanowski W. Crossvalidatory choice of the number of components from a principal component analysis. Technometrics. 1982;24:73-7.

43. Martens H, Naes T. Multivariate Calibration. Chichester: John Wiley and Sons; 1989. 504 p.

44. Kaplan E, Meier P. Nonparametric estimation from incomplete observations. J AM Stat Assn. 1958;53:457-81.

45. Mantel N. Evaluation of survival data and two new rank order statistics arising in its consideration. Cancer Chemother Rep. 1966;50(3):163-70.

REFERENCES

1. Alhatemi G, Aldiwani H, Alhatemi R, Hussein M, Mahdai S, Seyoum B. Glycemic control in the critically ill: Less is more. Cleve Clin J Med. 2022;89(4):191-9.

2. Plummer MP, Bellomo R, Cousins CE, Annink CE, Sundararajan K, Reddi BA, et al. Dysglycaemia in the critically ill and the interaction of chronic and acute glycaemia with mortality. Intensive Care Med. 2014;40(7):973-80.

3. Kitabchi AE, Umpierrez GE, Miles JM, Fisher JN. Hyperglycemic crises in adult patients with diabetes. Diabetes care. 2009;32(7):1335-43.

4. Bar-Or D, Rael LT, Madayag RM, Banton KL, Tanner A, 2nd, Acuna DL, et al. Stress Hyperglycemia in Critically Ill Patients: Insight Into Possible Molecular Pathways. Front Med (Lausanne). 2019;6:54.

5. Godinjak A, Iglica A, Burekovic A, Jusufovic S, Ajanovic A, Tancica I, et al. Hyperglycemia in Critically Ill Patients: Management and Prognosis. Med Arch. 2015;69(3):157-60.

6. Barton RN. Neuroendocrine mobilization of body fuels after injury. Br Med Bull. 1985;41(3):218-25.

7. Frayn KN, Little RA, Maycock PF, Stoner HB. The relationship of plasma catecholamines to acute metabolic and hormonal responses to injury in man. Circ Shock. 1985;16(3):229-40.

8. Memon RA, Feingold KR, Grunfeld C. Cytokines and intermediary metabolism. In: Remick DG, Friedland JS, editors. Cytokines in Health and Disease. 2nd ed. New York: Marcel Dekker; 1997. p. 381-99.

9. Sakurai Y, Zhang XJ, Wolfe RR. TNF directly stimulates glucose uptake and leucine oxidation, inhibiting FFA flux in conscious dogs. Am J Physiol. 1996;270(5 Pt 1): E 864-72.

10. Mehta VK, Hao W, Brooks-Worrell BM, Palmer JP. Low-dose interleukin 1 and tumor necrosis factor individually stimulate insulin release but in combination cause suppression. Eur J Endocrinol. 1994;130(2):208-14.

11. Esposito K, Nappo F, Marfella R, Giugliano G, Giugliano F, Ciotola M, et al. Inflammatory cytokine concentrations are acutely increased by hyperglycemia in humans: role of oxidative stress. Circulation. 2002;106(16):2067-72.

12. Jeschke MG, Klein D, Bolder U, Einspanier R. Insulin attenuates the systemic inflammatory response in endotoxemic rats. Endocrinology. 2004;145(9):4084-93.

13. Brix-Christensen V, Andersen SK, Andersen R, Mengel A, Dyhr T, Andersen NT, et al. Acute hyperinsulinemia restrains endotoxin-induced systemic inflammatory

response: an experimental study in a porcine model. Anesthesiology. 2004;100(4):861-70.

14. Sigurdsson MI, Kobayashi H, Amrein K, Nakahira K, Rogers AJ, Pinilla-Vera M, et al. Circulating N-formylmethionine and metabolic shift in critical illness: a multicohort metabolomics study. Crit Care. 2022;26(1):321.

15. Johnson CH, Ivanisevic J, Siuzdak G. Metabolomics: beyond biomarkers and towards mechanisms. Nat Rev Mol Cell Biol. 2016;17(7):451-9.

16. Langley RJ, Tsalik EL, van Velkinburgh JC, Glickman SW, Rice BJ, Wang C, et al. An integrated clinico-metabolomic model improves prediction of death in sepsis. Sci Transl Med. 2013;5(195):195ra95.

17. Langley RJ, Tipper JL, Bruse S, Baron RM, Tsalik EL, Huntley J, et al. Integrative "omic" analysis of experimental bacteremia identifies a metabolic signature that distinguishes human sepsis from systemic inflammatory response syndromes. Am J Respir Crit Care Med. 2014;190(4):445-55.

18. Kobayashi H, Amrein K, Lasky-Su JA, Christopher KB. Procalcitonin metabolomics in the critically ill reveal relationships between inflammation intensity and energy utilization pathways. Sci Rep. 2021;11(1):23194.

19. Amrein K, Schnedl C, Holl A, Riedl R, Christopher KB, Pachler C, et al. Effect of high-dose vitamin D3 on hospital length of stay in critically ill patients with vitamin D deficiency: the VITdAL-ICU randomized clinical trial. JAMA. 2014;312(15):1520-30.

20. Amrein K, Lasky-Su JA, Dobnig H, Christopher KB. Metabolomic basis for response to high dose vitamin D in critical illness. Clinical nutrition. 2021;40(4):2053-60.

21. Jacobi J, Bircher N, Krinsley J, Agus M, Braithwaite SS, Deutschman C, et al. Guidelines for the use of an insulin infusion for the management of hyperglycemia in critically ill patients. Crit Care Med. 2012;40(12):3251-76.

22. van Iterson M, t Hoen PA, Pedotti P, Hooiveld GJ, den Dunnen JT, van Ommen GJ, et al. Relative power and sample size analysis on gene expression profiling data. BMC Genomics. 2009;10:439.

23. Chong J, Xia J. Using MetaboAnalyst 4.0 for Metabolomics Data Analysis, Interpretation, and Integration with Other Omics Data. Methods Mol Biol. 2020;2104:337-60.

24. Le Gall JR, Lemeshow S, Saulnier F. A new Simplified Acute Physiology Score (SAPS II) based on a European/North American multicenter study. JAMA. 1993;270(24):2957-63.

25. Pinto J, Domingues MR, Galhano E, Pita C, Almeida Mdo C, Carreira IM, et al. Human plasma stability during handling and storage: impact on NMR metabolomics. Analyst. 2014;139(5):1168-77.

26. FitzMaurice GM, Laird NM, Ware JH. Applied longitudinal analysis. Hoboken, New Jersey: Wiley; 2011.

27. Benjamini Y, Hochberg Y. Controlling for false discovery rate: a practical and powerful approach to multiple testing. Journal of the Royal Statistical Society Series B (Methodological). 1995;57:289–300.

28. Bylesjö M, Rantalainen M, Cloarec O, Nicholson JK, Holmes E, Trygg J. OPLS discriminant analysis: combining the strengths of PLS-DA and SIMCA classification. Journal of Chemometrics. 2006;20(8-10):341–51.

29. Trygg J, Wold S. Orthogonal projections to latent structures (O-PLS). J Chemometrics. 2002;16:119–28.

30. Westerhuis JA, Hoefsloot HCJ, Smit S, Vis DJ, Smilde AK, van Velzen EJJ, et al. Assessment of PLSDA cross validation. Metabolomics 2008;4(1):81–9.

31. Eriksson L, Trygg J, Wold S. CV-ANOVA for significance testing of PLS and OPLS models. Journal of Chemometrics. 2008;22(11-12):594-600.

32. Eastment H, Krzanowski W. Crossvalidatory choice of the number of components from a principal component analysis. Technometrics. 1982;24:73-7.

33. Martens H, Naes T. Multivariate Calibration. Chichester: John Wiley and Sons; 1989. 504 p.

34. Kaplan E, Meier P. Nonparametric estimation from incomplete observations. J AM Stat Assn. 1958;53:457-81.

35. Mantel N. Evaluation of survival data and two new rank order statistics arising in its consideration. Cancer Chemother Rep. 1966;50(3):163-70.

36. Cahill GF, Jr. Fuel metabolism in starvation. Annu Rev Nutr. 2006;26:1-22.

37. Benedict FG. A Study of Prolonged Fasting. Washington, DC, USA: Carnegie Institute of Washington; 1915.

38. Felig P. Amino acid metabolism in man. Annual review of biochemistry. 1975;44:933-55.

39. Mizock BA. Alterations in fuel metabolism in critical illness: hyperglycaemia. Best Pract Res Clin Endocrinol Metab. 2001;15(4):533-51.

40. Green P, Theilla M, Singer P. Lipid metabolism in critical illness. Curr Opin Clin Nutr Metab Care. 2016;19(2):111-5.

41. Khovidhunkit W, Kim MS, Memon RA, Shigenaga JK, Moser AH, Feingold KR, et al. Effects of infection and inflammation on lipid and lipoprotein metabolism: mechanisms and consequences to the host. J Lipid Res. 2004;45(7):1169-96.

42. Van Wyngene L, Vandewalle J, Libert C. Reprogramming of basic metabolic pathways in microbial sepsis: therapeutic targets at last? EMBO Mol Med. 2018;10(8).

43. Eichmann TO, Lass A. DAG tales: the multiple faces of diacylglycerol--stereochemistry, metabolism, and signaling. Cellular and molecular life sciences: CMLS. 2015;72(20):3931-52.

44. Wattenberg BW, Raben DM. Diacylglycerol kinases put the brakes on immune function. Sci STKE. 2007;2007(398):pe43.

45. Wang YF, Lee GL, Huang YH, Kuo CC. sn-1,2-diacylglycerols protect against lethal endotoxemia by controlling systemic inflammation. Immunobiology. 2016;221(11):1309-18.

46. Chauveau A, Le Floc'h A, Bantilan NS, Koretzky GA, Huse M. Diacylglycerol kinase alpha establishes T cell polarity by shaping diacylglycerol accumulation at the immunological synapse. Sci Signal. 2014;7(340):ra82.

47. Tsuchiya R, Tanaka T, Hozumi Y, Nakano T, Okada M, Topham MK, et al. Downregulation of diacylglycerol kinase zeta enhances activation of cytokine-induced NF-kappaB signaling pathway. Biochim Biophys Acta. 2015;1853(2):361-9.

48. Noessner E. DGK-alpha: A Checkpoint in Cancer-Mediated Immuno-Inhibition and Target for Immunotherapy. Front Cell Dev Biol. 2017;5:16.

49. Xia P, Inoguchi T, Kern TS, Engerman RL, Oates PJ, King GL. Characterization of the mechanism for the chronic activation of diacylglycerol-protein kinase C pathway in diabetes and hypergalactosemia. Diabetes. 1994;43(9):1122-9.

50. van der Veen JN, Kennelly JP, Wan S, Vance JE, Vance DE, Jacobs RL. The critical role of phosphatidylcholine and phosphatidylethanolamine metabolism in health and disease. Biochim Biophys Acta Biomembr. 2017;1859(9 Pt B):1558-72.

51. Chang W, Hatch GM, Wang Y, Yu F, Wang M. The relationship between phospholipids and insulin resistance: From clinical to experimental studies. J Cell Mol Med. 2019;23(2):702-10.

52. Shinzawa-Itoh K, Aoyama H, Muramoto K, Terada H, Kurauchi T, Tadehara Y, et al. Structures and physiological roles of 13 integral lipids of bovine heart cytochrome c oxidase. EMBO J. 2007;26(6):1713-25.

53. Ichimura Y, Kirisako T, Takao T, Satomi Y, Shimonishi Y, Ishihara N, et al. A ubiquitin-like system mediates protein lipidation. Nature. 2000;408(6811):488-92.

54. Patel D, Witt SN. Ethanolamine and Phosphatidylethanolamine: Partners in Health and Disease. Oxid Med Cell Longev. 2017;2017:4829180.

55. Yang WS, Stockwell BR. Ferroptosis: Death by Lipid Peroxidation. Trends Cell Biol. 2016;26(3):165-76.

56. D'Herde K, Krysko DV. Ferroptosis: Oxidized PEs trigger death. Nat Chem Biol. 2017;13(1):4-5.

57. Vickers AJ. How many repeated measures in repeated measures designs? Statistical issues for comparative trials. BMC Med Res Methodol. 2003;3:22.

58. Frison L, Pocock SJ. Repeated measures in clinical trials: analysis using mean summary statistics and its implications for design. Stat Med. 1992;11(13):1685-704.

59. Fang H, Brooks GP, Rizzo ML, Espy KA, Barcikowski RS. A Monte Carlo Power Analysis of Traditional Repeated Measures and Hierarchical Multivariate Linear Models in Longitudinal Data Analysis. J Mod Appl Stat Methods. 2008;7(1).

60. Mei Y, Kim BS, Tsui K. Linear mixed effects models for feature selection in high dimensional NMR spectra. Exprt Syst Applic. 2009;36:4703–8.

61. Ernest B, Gooding JR, Campagna SR, Saxton AM, Voy BH. MetabR: an R script for linear model analysis of quantitative metabolomic data. BMC Res Notes. 2012;5:596.

62. Kelly RS, Croteau-Chonka DC, Dahlin A, Mirzakhani H, Wu AC, Wan ES, et al. Integration of metabolomic and transcriptomic networks in pregnant women reveals biological pathways and predictive signatures associated with preeclampsia. Metabolomics. 2017;13(1).

63. Lee-Sarwar K, Kelly RS, Lasky-Su J, Kachroo P, Zeiger RS, O'Connor GT, et al. Dietary and Plasma Polyunsaturated Fatty Acids Are Inversely Associated with Asthma and Atopy in Early Childhood. J Allergy Clin Immunol Pract. 2019;7(2):529-38 e8.

64. Chary S, Amrein K, Mahmoud SH, Lasky-Su JA, Christopher KB. Sex-Specific Catabolic Metabolism Alterations in the Critically Ill following High Dose Vitamin D. Metabolites. 2022;12(3).

65. Dunn WB, Lin W, Broadhurst D, Begley P, Brown M, Zelena E, et al. Molecular phenotyping of a UK population: defining the human serum metabolome. Metabolomics. 2015;11(1):9-26.

MANUSCRIPT 2

Chronic Diseases and Metabolic Homeostasis Derangement in Critical Illness: A Post-hoc Metabolomics cohort study

Authors: Sigma Hossain, MBBS, MSc, MSc, MPhil, MPH[1,4], Karin Amrein, MD, MSc[2], Jessica A. Lasky-Su, ScD[3], Kenneth B. Christopher, MD, SM[3,4]

Affiliations:

1. Harvard Medical School, Boston, USA
5. Division of Endocrinology and Diabetology, Medical University of Graz, Graz, Austria
6. Jessica A. Lasky-Su, ScD, Channing Division of Network Medicine, Brigham and Women's Hospital, USA
7. Division of Renal Medicine, Channing Division of Network Medicine, Brigham and Women's Hospital, USA

Corresponding Author: Kenneth B. Christopher, MD, SM, Division of Renal Medicine, Channing Division of Network Medicine, Brigham, and Women's Hospital, 75 Francis Street, Boston, MA 02115 USA. E-mail: kbchristopher@bwh.harvard.edu Tel: 617-272-0535

Acknowledgment: This manuscript is dedicated to the memory of our dear friend and colleague Nathan Edward Hellman, MD, Ph.D.

Author's contributions: Conceptualization: S.H., K.A., J.L-S., K.C.; Methodology: S.H., K.A., J.L-S., K.C.; Software: J.L-S., K.C.; Formal analysis: S.H., K.C.;

Investigation: K.A., K.C.: Resources: K.A., J.L-S., K.C.; Data Curation: S.H., K.A., J.L-S., K.C.; Writing-Original Draft: S.H., K.A., J.L-S., K.C.; Writing- Review & Editing: S.H., K.A., J.L-S., K.C.; Data Visualization: S.H., J.L-S., K.C; Supervision: J.L-S., K.C; Project Administration & Funding acquisition: K.A.& K.C.

Financial/non-financial disclosures: Dr. Amrein reports receiving lecture fees from Fresenius Kabi. Drs. Hossain, Lasky-Su, and Christopher report no financial or other relationships that might lead to a conflict of interest

Funding: This work was supported by the National Institutes of Health [R01 GM115774]. The European Society supported the VITdAL-ICU trial for Clinical Nutrition and Metabolism (ESPEN), a research grant including the provision of study medication from Fresenius Kabi (Germany), and the Austrian National Bank (Jubiläumsfonds, Project Nr. 14143).

Running Head: Chronic Diseases and Metabolic Homeostasis Derangement in Critical Illness

Total word count: 2665

ABSTRACT

Background: Critical illness frequently results in loss of metabolic homeostasis characterized by a significant disturbance of many metabolic processes. The co-existing chronic medical conditions can impact the severity of the acute illness, the types and amount of treatment given, and the outcomes in the intensive care unit.

Objective: To find out the association between chronic comorbidities and plasma metabolites over the first week of critical illness using the updated Charlson Comorbidity Index (uCCI)

Methods: This was a post-hoc metabolomics cohort study of blood samples from the VITdAL-ICU trial where subjects received a high dose of vitamin D3 or a placebo. Exposure was measured in uCCI. A total of 983 metabolites from 1209 plasma samples of 421 patients were analyzed. Mixed-effects modeling was used to study metabolite changes over time relative to uCCI < or ≥ 4 adjusted for age, sex, SAPS II score, sepsis, intubation, and ICU type.

Results: There was a significantly worse survival with uCCI≥ 4 (log-rank P<0.001). Significant crude differences existed in day 0 plasma samples in 430 individual metabolites in subjects with uCCI<4 or uCCI≥ 4 group. In the repeated measure metabolomics data, significant metabolomics difference was observed with increasing uCCI where several metabolites significantly increased, e.g., Branched-chain amino acids (BCAA), Short-chain acylcarnitines, purine nucleotides {1-methyladenosine (m1A), N2, N2-dimethylguanosine (m22G)} and pentose phosphate pathway activation. In contrast, several metabolites were significantly decreased, e.g., Sphingomyelin.

Conclusion: In critically ill patients, chronic disease is associated with differential utilization of energy pathways.

Word counts: 244

Keywords: Critical illness, Chronic Diseases, updated Charlson Comorbidity Index (uCCI)

List of non-standard abbreviations: VITdAL-ICU trial- Correction of Vitamin D Deficiency in Critically Ill Patients trial; OPLS-DA- Orthogonal partial least square-discriminant analysis; CV- ANOVA- Cross-validation analysis of variance, SAPS- Simplified Acute Physiology Scores

INTRODUCTION

In the critically ill, it is unclear which underlying factors contribute to the heterogeneity in response to acute illness, which may relate to differences in genetic susceptibility, chronic comorbidity, or treatment response (1). Critically ill patients frequently have coexisting chronic medical diseases, which can affect the severity of the acute illness, the types and amount of treatment provided, and influence adverse outcomes (2). Critical illness outcomes are likely driven by the severity of organ dysfunction, comorbidity, and multimorbidity (2, 3). In addition, critical illness frequently results in the loss of metabolic homeostasis, marked by the severe disruption of numerous metabolic processes, including energy production and utilization (4, 5).

Metabolomics encompasses the systematic identification and quantification of all metabolic products of a biological system at a specific point in time (6). Metabolomics can offer a comprehensive strategy for comprehending an organism's phenotype because metabolites serve as endpoints of gene expression and cell activity (7). Analyzing the blood metabolome generates a highly coordinated profile of metabolic homeostasis (8). Critical illness frequently results in the loss of metabolic homeostasis, which is marked by the severe disruption of numerous metabolic processes (4).

The Charlson comorbidity index (CCI) is a frequently used tool that classifies or weights comorbid illnesses to predict mortality. Recently, Quan et al. updated the conditions and weights included in the CCI, simplifying the score to 12 comorbidities and validating an

updated CCI (uCCI) to predict 1-year mortality after hospital discharge (9). The uCCI is a more refined, parsimonious prognostic mortality score than the CCI and has been used in critical illness studies on Staphylococcus aureus bacteremia and burn injury (10, 11).

Plasma metabolomics studies in critical illness show a consistent alteration of metabolism linked to acute illness severity and outcome prediction (12). But the importance of energy utilization pathways among critically ill patients with comorbidities is unknown. Therefore, we performed a post-hoc metabolomics cohort study of 1209 plasma samples collected over 7 days from 421 subjects enrolled in the VITdAL-ICU trial with uCCI determined (13). We hypothesized that a higher chronic disease burden, as assessed by uCCI, is associated with differential energy utilization pathways in critically ill adult patients. Therefore, we investigated the uCCI among the VITdAL-ICU trial subjects to determine the association between chronic comorbidities and 983 individual plasma metabolite abundance over the first week of critical illness.

METHODS

We performed a post-hoc metabolomics cohort study of plasma samples from the VITdAL-ICU trial (NCT01130181), a placebo-controlled, double-blind, single-center trial conducted in 5 medical and surgical intensive care units in southeast Austria (13). This trial included 492 critically ill adult subjects with 25(OH)D < 20 ng/mL randomly allocated to placebo or vitamin D3 once at a dose of 540,000 IU followed by 90,000 IU

monthly. The Medical University of Graz and the Austrian Agency for Health and Food Safety approved the trial. At VITdAL-ICU trial enrollment, written informed consent was obtained following Austrian and European Union requirements and the principles of the Declaration of Helsinki (14). Consent included permission for plasma specimens to be saved for future research studies. The post-hoc study research protocol was approved by the Mass General Brigham Human Research Committee Institutional Review Board at the Brigham and Women's Hospital (Protocol # 2015P002766).

Frozen plasma from 453 trial participants before randomization was available for metabolomics analysis. Twenty-five patients who did not have multiple plasma time points available for analysis were excluded. An additional 7 subjects who did not have data for uCCI determination were excluded, leaving an analytic cohort of 421 subjects (Supplemental Figure 1). Clinical trial data included age, biological sex, Simplified Acute Physiology Score (SAPS) II, admission diagnosis category, baseline serum 25(OH)D levels, and uCCI. Admission diagnosis category was determined at ICU admission by trial investigators as Neurosurgery, Cardiac surgery, Cardiovascular, Gastrointestinal/liver, Hematologic/Oncology/ Metabolic, Neurologic, Other non-operative, Other operatives, Renal, Respiratory, Sepsis/infectious, Thoracic Surgery, Transplantation, Trauma, and Vascular Surgery.

Blood samples were collected between May 2010 and March 2012 from VITdAL-ICU trial subjects on days 0, 3, and 7. Fractionated plasma was aliquoted, stored at -80°C,

thawed once, and analyzed in 2017 using four ultra-high-performance liquid chromatography/tandem accurate mass spectrometry methods by Metabolon, Inc (NC, USA) (13). A total of 983 metabolites from 1209 plasma samples of 421 patients were analyzed. Individual metabolite raw area count data was normalized, cube root transformed, and Pareto scaled to produce abundance data on the same scale and with an approximately normal distribution (15, 16).

The exposure of interest was the Updated Charlson Comorbidity Index (uCCI) dichotomized as uCCI < or ≥ 4 based on prior work by others (10). The primary outcome was individual metabolite relative abundance determined by liquid chromatography coupled mass spectrometry. Metabolite abundance is defined as the total ion count for the given mass-to-charge ratio (m/z) assigned to the particular metabolite (17). The secondary outcome was all-cause 180-day mortality determined by hospital records and telephone follow-up. Distributions of and differences in crude survival between uCCI groups were determined via the Kaplan-Meier survival curve and the log-rank test, respectively (18, 19).

The study sample size was determined via MetaboAnalyst with a false discovery rate (FDR) corrected alpha of 0.05 using equations for single time point metabolomics data with binary uCCI groups (20, 21). To achieve 80% power, our study requires a sample of 150 subjects in each group (20). In addition, analysis of repeated plasma metabolomics data is known to increase study power (22) substantially.

All data were analyzed in a complete case analysis fashion. For univariate analysis of day 0 data, Student's t-test was used to identify metabolites that are associated with a dichotomized uCCI (uCCI < or ≥ 4) applying a false discovery rate adjusted p-value (q-value) threshold of 0.05 using MetaboAnalyst (21, 23). Data from day 0 were also analyzed using orthogonal partial least squares discriminant analysis (OPLS-DA), a supervised method for determining the significance of classification discrimination (SIMCA 15.0 Umetrics, Umea, Sweden) (24). OPLS-DA is a statistical modeling tool that provides insights into metabolite differences between subjects grouped by uCCI (25). Permutation testing was performed for model validation (26, 27). A seven-fold cross-validation analysis of variance (CV-ANOVA) was utilized to determine model significance (27).

For day 0 data in 421 subjects, correlations between uCCI groups (exposure) and individual metabolite abundance (outcome) were determined utilizing linear regression models corrected for age, sex, baseline 25(OH)D, SAPS II, and admission diagnosis category. For repeated measures data in 421 subjects, the association between uCCI groups (exposure) and relative abundance of individual metabolites (outcome) at day 0, 3, and 7 were determined utilizing mixed effects linear regression adjusted for age, sex, SAPS II, admission diagnosis category, sample day, 25(OH)D at day 0, and change in 25(OH)D from day 0-3 with an individual subject-specific random-intercept. All linear regression and mixed-effects models were analyzed using STATA 16.1MP (28). A Benjamini–Hochberg procedure false discovery rate q-value threshold of 0.05 was used to identify all significant associations (23).

RESULTS

Baseline characteristics of the analytic cohort were not significantly different between subjects grouped by uCCI for biological sex, SAPS II score, sepsis, intubation, and ICU type. Patients in the uCCI<4 groups were significantly younger than patients in uCCI≥ 4 groups. Significant differences existed with respect to age, uCCI, and ICU type **(Table 1, Supplementary Table S1)**. The overall 180-day mortality of the 421-subject analytic cohort was 36.8%. The 180-day mortality among patients with uCCI<4 was 26.8% and 47.8% in the uCCI≥4 groups ($\chi 2(1) = 19.8$; $P < 0.001$). There was significantly worse survival with uCCI≥ 4 (log-rank P<0.001, **Figure 1**).

Single time point data

In t-test analyses, significant metabolite differences exist between the uCCI groups **(Table 2).** In day 0 plasma samples (N=421), significant differences exist in 430 individual metabolites (q-value threshold of 0.05), including increases in branched-chain amino acids, short-chain acylcarnitines, modified nucleosides (1-methyladenosine, N2, N2-dimethylguanosine) and pentose phosphate pathway metabolites and decrease in sphingomyelins between the uCCI groups.

Concerning subject metabolomic profiles at day 0, though the multivariable OPLS-DA models had poor predictability (Q2<0.3), the permutation test confirmed the stability and robustness of the model with negative permutation Q2 y-axis intercepts (-0.458) indicating model validity **(Table 3)** (26, 27, 29). Furthermore, the cross-validation

procedure showed that the uCCI groups at day 0 were significantly separated (CV-ANOVA p value < 0.001). Figure 2 illustrates the separation of circulating metabolomes from individual patients at day 0 with uCCI<4 or uCCI≥ 4.

In the linear regression analysis, there were significant associations at day 0 between the abundance of 297 individual metabolites (q-value<0.05) and uCCI≥4 following adjustment for age, sex, baseline 25(OH)D, SAPS II, admission diagnosis category, and baseline 25(OH)D. Metabolites associated with increased uCCI≥4 at day 0 included elevated modified nucleosides (1-methyladenosine (m1A), N2, N2-dimethylguanosine (m22G)), BCAA metabolites, short-chain acylcarnitines, metabolites of the pentose phosphate pathway and decreased sphingomyelin species **(Table 4).**

Multiple time point data

In mixed effects modeling of 1209 total day 0, 3, and 7 plasma samples from the analytic cohort (N=421), 230 metabolites had significantly positive (q-value<0.05) associations with uCCI≥4 dominated by increases in modified nucleosides (m1A, m22G), BCAA metabolites, short-chain acylcarnitines and metabolites of the pentose phosphate pathway (Highlighted in Table 2, Full data in Supplemental Data A). Thirty-one metabolites had significant negative associations with uCCI≥4, primarily by sphingomyelin decreases **(Table 5)**. Similar metabolite patterns were observed in mixed effects models with additional adjustment for creatinine at day 0 (Data not shown).

DISCUSSION

The present study aimed to determine the association between chronic comorbidities and plasma metabolites over the first week of critical illness using the updated Charlson comorbidity index (uCCI). Significant differences in metabolomics profiles were observed with an elevated uCCI≥4 with substantial increases in branched-chain amino acids (BCAAs), short-chain acylcarnitines, modified nucleosides, and pentose phosphate pathway metabolites. In contrast, several sphingomyelin species are decreased in subjects with uCCI≥4. This study highlighted the alteration of metabolomics during critical illness in patients with comorbidities.

Critical illness releases free fatty acids (FAA) and branched-chain amino acids (BCAAs) metabolites into circulation due to the catabolism of adipose and muscle tissue. BCAAs, fatty acids, and the intermediate metabolites produced during their catabolism play a crucial role as metabolic substrates in numerous physiological processes, including inflammation, energy metabolism, and mitochondrial biogenesis. During the mitochondrial fatty acid β-oxidation impairment associated with critical illness, the liver catabolizes BCAAs to high-energy compounds reflecting a metabolic switch (5, 30). Short-chain acylcarnitines are considered the most abundant acylcarnitines in the body, accounting for nearly 80% or more of total acylcarnitines in plasma (31). In the critically ill, increased circulating plasma short-chain acylcarnitines (C2-C7) indicates compromised mitochondrial fatty acid β-oxidation and reflects a decrease in

mitochondrial energy production indicative of a metabolic shift (32). Further, the observed elevated C3- and C5-acylcarnitines are known to be derived from BCAA metabolites (33).

Our study also found a significantly increased modified nucleoside abundance (m1A, m22G) with increased comorbidities. Circulating modified nucleosides reflect whole-body RNA turnover and may indicate cell stress (34-36). Circulating levels of m1A are shown to be increased in response to experimental models of oxidative stress (37). Further, strong associations between m22G and all-cause mortality exist in adults with diabetes (38). Critically ill patients with comorbidities may be more susceptible to cellular damage due to oxidative stress, which may account for our observed increases in modified nucleosides with uCCI ≥4.

We observed a significant increase in the pentose phosphate pathway metabolites with uCCI ≥4. The pentose phosphate pathway is essential for redox balance because it produces NADPH via an oxidative branch and nucleic acid via a non-oxidative branch (39). In critical illness, the pentose phosphate pathway acts as a “metabolic redox sensor” upregulated during oxidative stress (40, 41). Transcriptomic profiling of whole blood in critically ill patients revealed increased activity in the oxidative branch of the pentose phosphate pathway, indicating a metabolic shift away from mitochondrial beta-oxidation (42). The observed increases of purine nucleotides, short-chain acylcarnitines,

BCAA catabolic metabolites, and pentose phosphate pathway metabolites with more significant comorbidities are thus indicative of a metabolic shift.

Sphingomyelins are essential for plasma membrane function and act as signaling mediators of inflammation and cellular stress. Sphingomyelin synthases play crucial roles in biological functions such as cell migration, apoptosis, autophagy, and cell survival/proliferation, as well as in human diseases such as cancer and cardiovascular disease (43). Hydrolyzation of sphingomyelins to ceremide is activated by oxidative stress, TNF-α, IL-1β, and Fas ligand (44). Thus, it is most likely that our observation of low plasma sphingomyelin species in critically ill patients with uCCI≥4 is related to inflammation and may contribute to disruption in homeostasis.

Our study approach has several strengths. First, using many plasma samples at multiple time points early in critical illness allows for a dynamic view of critical illness metabolomics related to chronic disease. Second, repeated measures in individual patients decrease intra-patient variability, thus increasing statistical power (45-48). Third, our adjustment for the absolute change in 25(OH)D level at day 3 mitigates the effect of vitamin D intervention on the observed metabolomic changes, allowing for the study of the entire analytic cohort (49, 50). Finally, linear mixed models are extremely useful for metabolomic data measured at multiple time points as they remove confounding variables with a fixed effect (e.g., age, sex, SAPS II) and those with a random effect (e.g., patient) (51, 52). For multiple testing correction, a false discovery rate adjusted p-value (q-value) threshold of 0.05 was used to identify all significant differences (23).

We do acknowledge potential limitations to our approach. First, our cohort population was White from a single large academic medical center which may limit generalizability to all critically ill. Though our data was generated from a randomized trial, we could not exclude the effect of unknown confounders despite multivariable adjustment because of nonrandomized comparisons of metabolite abundance. Despite adjustment for biological sex, the results may be driven by unmeasured confounders related to differences between men and women (53). Additionally, we cannot study racial disparities in metabolomics as the subjects studied were all White (54). Lastly, as our study is post-hoc, our inferences require external validation and should be considered hypothesis-generating.

CONCLUSIONS

With increased chronic disease determined by the uCCI, there was a noticeable shift in the metabolome: some metabolites significantly increased, such as BCAA, short-chain acylcarnitines, purine nucleotides, and pentose phosphate pathway activity, while sphingomyelin species significantly decreased. Single biomarkers cannot accurately measure the complexity of critical illnesses. Integrating metabolomics and disease severity may create a more nuanced understanding of the dysregulation of metabolic homeostasis in critical illness.

FIGURE LEGENDS

Figure 1. Kaplan–Meier Estimates of Survival. Kaplan–Meier estimates of overall survival by uCCI (N=421). The log-rank test revealed a significant difference in survival between the uCCI groups (P=0.001). The blue line indicates uCCI <4 groups and the red line indicates uCCI ≥ 4 group

Figure 2. OPLS-DA score Plot. t1: The predicted principal components-score value of main components and the difference between uCCI <4 and uCCI ≥ 4, t01: Orthogonal principal component-score value of orthogonal components and difference in the observation group. Green circles represent the metabolome of individual subjects with uCCI <4; Blue circles represent the metabolome of individual subjects with uCCI ≥ 4.

Table 1. Cohort Characteristics (N= 421)

Baseline Characteristics	Total	uCCI < 4	uCCI ≥ 4	P-value
No.	421	220	201	
Age Mean (SD)	64.2 (15.0)	61.6 (16.9)	67.1 (12.0)	**<0.001**
Female Sex No. (%)	149 (38)	84 (32)	65 (44)	0.21
Non-White No. (%)	0 (0)	0 (0)	0 (0)	
Updated uCCI Mean (SD)	3.5 (3.2)	1.0 (1.1)	6.4 (2.2)	**<0.001**
SAPS II Mean (SD)	33.3 (15.4)	32.6 (15.6)	34.1 (15.1)	0.34
Sepsis No. (%)	31 (7)	11 (5)	20 (10)	0.052
Intubation No. (%)	279 (66)	142 (65)	137 (68)	0.43
ICU				0.01
Anesthesia ICU No. (%)	81 (19)	46 (21)	35 (17)	
Cardiac Surgery ICU No. (%)	123 (29)	61 (28)	62 (31)	
Surgical ICU No. (%)	22 (5)	8 (4)	14 (7)	
Medical ICU No. (%)	89 (21)	37 (17)	52 (26)	
Neurological ICU No. (%)	106 (25)	68 (31)	38 (19)	
180 days mortality No.(%)	154(36.8)	59(26.8)	96(47.8)	**<0.001**

Table 2. Crude Metabolite abundance differences in patients with uCCI ≥ 4 relative to those with uCCI < 4

Biochemical	t-stat	FDR	Super Pathway	Sub Pathway
2-hydroxy-3-methylvalerate	2.518	0.030672	Amino Acid	BCAA Metabolism
beta-hydroxyisovalerate	2.8186	0.014226	Amino Acid	BCAA Metabolism
3-hydroxy-2-ethyl propionate	2.8269	0.013948	Amino Acid	BCAA Metabolism
methylmalonate (MMA)	3.225	0.0044971	Lipid	BCAA Metabolism
isobutyrylglycine (C4)	3.7096	0.00097396	Amino Acid	BCAA Metabolism
ethyl malonate	4.2395	0.00014457	Amino Acid	BCAA Metabolism
N-acetylleucine	4.2773	0.00012702	Amino Acid	BCAA Metabolism
N-acetyl isoleucine	4.4542	6.39E-05	Amino Acid	BCAA Metabolism
isovalerylglycine	4.6619	2.87E-05	Amino Acid	BCAA Metabolism
2,3-dihydroxy-2-methyl butyrate	4.6638	2.86E-05	Amino Acid	BCAA Metabolism
methylsuccinate	4.9404	9.14E-06	Amino Acid	BCAA Metabolism
N-acetylvaline	5.824	2.08E-07	Amino Acid	BCAA Metabolism
3-methylglutaconate	6.5476	4.94E-09	Amino Acid	BCAA Metabolism
ribitol	7.2621	1.44E-10	Carbohydrate	Pentose Metabolism
arabonate/xylonate	7.1013	2.79E-10	Carbohydrate	Pentose Metabolism
ribonate (ribonolactone)	6.8874	8.53E-10	Carbohydrate	Pentose Metabolism
arabinose	6.5698	4.57E-09	Carbohydrate	Pentose Metabolism
arabitol/xylitol	5.6484	4.38E-07	Carbohydrate	Pentose Metabolism
ribulonate/xylulonate*	4.8912	1.12E-05	Carbohydrate	Pentose Metabolism
sedoheptulose	3.7636	0.00080492	Carbohydrate	Pentose Metabolism
xylose	3.1001	0.0065082	Carbohydrate	Pentose Metabolism
N1-methyl inosine	7.8725	9.81E-12	Nucleotide	Purine Metabolism
N2,N2-dimethyl guanosine	7.7673	1.08E-11	Nucleotide	Purine Metabolism
acetylcarnitine (C2)	4.0756	0.00026043	Lipid	Short-chain Acylcarnitine
malonylcarnitine (C3-DC)	5.5339	7.22E-07	Lipid	Short-chain Acylcarnitine
3-hydroxybutyrylcarnitine (C3-DC)	4.6832	2.69E-05	Lipid	Short-chain Acylcarnitine
propionylcarnitine (C3)	3.803	0.00070265	Lipid	Short-chain Acylcarnitine
2-methylmalonylcarnitine (C4-DC)	5.5442	6.93E-07	Lipid	Short-chain Acylcarnitine
succinylcarnitine (C4-DC)	5.5041	7.98E-07	Energy	Short-chain Acylcarnitine
adipoylcarnitine (C6-DC)	5.3061	1.90E-06	Lipid	Short-chain Acylcarnitine
iso butyryl carnitine (C4)	3.3828	0.0027975	Amino Acid	Short-chain Acylcarnitine
butyryl carnitine (C4)	2.9159	0.01103	Lipid	Short-chain Acylcarnitine
tiglyl carnitine (C5)	4.8572	1.27E-05	Amino Acid	Short-chain Acylcarnitine
glutaroylcarnitine (C5)	4.466	6.13E-05	Amino Acid	Short-chain Acylcarnitine
2-methylbutyroylcarnitine (C5)	4.4577	6.33E-05	Amino Acid	Short-chain Acylcarnitine
isovalerylcarnitine (C5)	3.8499	0.00059247	Amino Acid	Short-chain Acylcarnitine
3-methylglutarylcarnitine (C6-DC)	5.328	1.71E-06	Amino Acid	Short-chain Acylcarnitine

hexanoylcarnitine (C6)	4.6706	2.80E-05	Lipid	Short-chain Acylcarnitine
3-methyladipoylcarnitine (C7-DC)	6.5651	4.57E-09	Lipid	Short-chain Acylcarnitine

Table 3. Day 0 OPLS-DA model goodness of fit, predictive ability, and model significance

	OPLS-DA			Permutation (*n* = 200)		CV-ANOVA
Classification Model	R2X	R2Y	Q2	R2 intercept (*x*-axis, *y*-axis)	Q2 intercept (*x*-axis, *y*-axis)	P-Value
uCCI<4 VS uCCI≥ 4	0.327	1.00	0.0664	0.00, 0.578	0.00, -0.458	0.0048

Table 4. Day 0 Metabolites significantly different in patients with uCCI ≥ 4 relative to those with uCCI < 4

Biochemical	Beta	FDR q-value	Super Pathway	Sub Pathway
3-methylglutaconate	0.309899002	3.68E-07	Amino Acid	BCAA Metabolism
isovalerylglycine	0.265608773	2.56E-04	Amino Acid	BCAA Metabolism
methyl succinate	0.233539737	2.46E-04	Amino Acid	BCAA Metabolism
2,3-dihydroxy-2-methyl-butyrate	0.197240281	1.99E-03	Amino Acid	BCAA Metabolism
N-acetylvaline	0.19164627	1.85E-05	Amino Acid	BCAA Metabolism
N-acetylleucine	0.188387175	1.20E-03	Amino Acid	BCAA Metabolism
isobutyrylglycine (C4)	0.188226058	3.34E-03	Amino Acid	BCAA Metabolism
ethyl malonate	0.161097954	2.41E-03	Amino Acid	BCAA Metabolism
N-acetyl isoleucine	0.150129787	2.04E-03	Amino Acid	BCAA Metabolism
2-hydroxy-3-methyl valerate	0.121274513	4.60E-02	Amino Acid	BCAA Metabolism
arabonate/xylonate	0.288515977	6.82E-08	Carbohydrate	Pentose Metabolism
arabinose	0.264196066	7.02E-07	Carbohydrate	Pentose Metabolism
ribonate (ribonolactone)	0.257535202	6.82E-08	Carbohydrate	Pentose Metabolism
arabitol/xylitol	0.243105598	6.36E-06	Carbohydrate	Pentose Metabolism
ribitol	0.220936931	5.29E-08	Carbohydrate	Pentose Metabolism
ribulonate/xylulonate*	0.189391287	1.29E-04	Carbohydrate	Pentose Metabolism
sedoheptulose	0.169216073	5.49E-03	Carbohydrate	Pentose Metabolism
xylose	0.133324007	3.11E-02	Carbohydrate	Pentose Metabolism
1-methyladenosine	0.188939397	1.12E-07	Nucleotide	Purine Metabolism
N2,N2-dimethyl guanosine	0.347048167	8.03E-09	Nucleotide	Purine Metabolism
acetylcarnitine (C2)	0.135251838	7.09E-03	Lipid	Short-chain Acylcarnitine
3-hydroxybutyrylcarnitine (C3-DC)	0.196803698	1.82E-03	Lipid	Short-chain Acylcarnitine
propionylcarnitine (C3)	0.135427832	1.12E-02	Lipid	Short-chain Acylcarnitine
2-methyl malonyl carnitine (C4-DC)	0.251603829	4.97E-05	Lipid	Short-chain Acylcarnitine
succinyl carnitine (C4-DC)	0.206695918	3.09E-05	Energy	Short-chain Acylcarnitine

iso butyryl carnitine (C4)	0.141274024	3.66E-02	Amino Acid	Short-chain Acylcarnitine
butyryl carnitine (C4)	0.120558359	4.66E-02	Lipid	Short-chain Acylcarnitine
tiglyl carnitine (C5)	0.183521191	6.62E-04	Amino Acid	Short-chain Acylcarnitine
2-methylbutyroylcarnitine (C5)	0.17164447	2.73E-03	Amino Acid	Short-chain Acylcarnitine
glutaroylcarnitine (C5)	0.156371259	3.24E-03	Amino Acid	Short-chain Acylcarnitine
isovalerylcarnitine (C5)	0.152330922	6.64E-03	Amino Acid	Short-chain Acylcarnitine
adipoylcarnitine (C6-DC)	0.280492143	4.70E-05	Lipid	Short-chain Acylcarnitine
3-methylglutarylcarnitine (C6-DC)	0.257171457	1.27E-04	Amino Acid	Short-chain Acylcarnitine
hexanoylcarnitine (C6)	0.181692502	1.07E-03	Lipid	Short-chain Acylcarnitine
3-methyladipoylcarnitine (C7-DC)	0.301407197	1.23E-06	Lipid	Short-chain Acylcarnitine
sphingomyelin (d18:1/17:0, d17:1/18:0, d19:1/16:0)	-0.109698615	1.16E-02	Lipid	Sphingomyelins
sphingomyelin (d17:1/14:0, d16:1/15:0)*	-0.111207788	4.85E-02	Lipid	Sphingomyelins
stearoyl sphingomyelin (d18:1/18:0)	-0.111970659	5.71E-03	Lipid	Sphingomyelins
sphingomyelin (d18:2/18:1)*	-0.114468561	5.84E-03	Lipid	Sphingomyelins
sphingomyelin (d18:1/22:1, d18:2/22:0, d16:1/24:1)*	-0.115396291	2.76E-03	Lipid	Sphingomyelins
sphingomyelin (d18:1/18:1, d18:2/18:0)	-0.129650535	1.23E-03	Lipid	Sphingomyelins
sphingomyelin (d18:2/21:0, d16:2/23:0)*	-0.131742914	6.44E-03	Lipid	Sphingomyelins
behenoyl sphingomyelin (d18:1/22:0)*	-0.138759323	8.97E-04	Lipid	Sphingomyelins
sphingomyelin (d18:1/20:1, d18:2/20:0)*	-0.145687451	3.46E-04	Lipid	Sphingomyelins
sphingomyelin (d18:1/20:0, d16:1/22:0)*	-0.150367073	2.19E-04	Lipid	Sphingomyelins
sphingomyelin (d18:2/23:0, d18:1/23:1, d17:1/24:1)*	-0.153721161	2.70E-03	Lipid	Sphingomyelins
lignoceroyl sphingomyelin (d18:1/24:0)	-0.161244194	7.13E-04	Lipid	Sphingomyelins

sphingomyelin (d18:1/19:0, d19:1/18:0)*	-0.16597711	5.00E-04	Lipid	Sphingomyelins
sphingomyelin (d18:1/25:0, d19:0/24:1, d20:1/23:0, d19:1/24:0)*	-0.178605056	3.83E-04	Lipid	Sphingomyelins
sphingomyelin (d18:1/21:0, d17:1/22:0, d16:1/23:0)*	-0.202948571	1.54E-04	Lipid	Sphingomyelins
tricosanoyl sphingomyelin (d18:1/23:0)*	-0.211631143	2.62E-05	Lipid	Sphingomyelins

Note: Significant results were presented following individual mixed effects modeling of each of the 983 individual metabolites measured at day 0. All estimates were adjusted for age, sex, SAPS II, admission diagnosis, and 25(OH)D at randomization. A multiple test-corrected thresholds of $q < 0.05$ was used to identify all significant associations. Positive β coefficient values indicate higher metabolite abundance with increasing day 0 serum glucose.

Table 5. Metabolites significantly different in patients with uCCI ≥ 4 relative to those with uCCI < 4 over day 0, 3 and 7

Biochemical	Beta	FDR q-value	Super Pathway	Sub Pathway
3-methylglutaconate	0.299294578	6.35E-08	Amino Acid	BCAA Metabolism
isovalerylglycine	0.253345563	2.09E-05	Amino Acid	BCAA Metabolism
methyl succinate	0.237096199	5.63E-07	Amino Acid	BCAA Metabolism
2,3-dihydroxy-2-methyl butyrate	0.225136632	8.32E-06	Amino Acid	BCAA Metabolism
N-acetylvaline	0.190340239	8.68E-08	Amino Acid	BCAA Metabolism
isobutyrylglycine (C4)	0.185299368	4.04E-04	Amino Acid	BCAA Metabolism
N-acetylleucine	0.177033429	4.75E-06	Amino Acid	BCAA Metabolism
N-acetyl isoleucine	0.169580161	1.57E-06	Amino Acid	BCAA Metabolism
ethyl malonate	0.163570783	4.43E-04	Amino Acid	BCAA Metabolism
methylmalonate (MMA)	0.12701982	1.20E-02	Lipid	BCAA Metabolism
beta-hydroxy isovalerate	0.1051646	1.67E-02	Amino Acid	BCAA Metabolism
2-hydroxy-3-methyl valerate	0.100864754	2.40E-02	Amino Acid	BCAA Metabolism
3-hydroxy-2-ethyl propionate	0.090782797	2.23E-02	Amino Acid	BCAA Metabolism
arabonate/xylonate	0.29100864	7.50E-10	Carbohydrate	Pentose Metabolism
ribitol	0.24933947	3.05E-10	Carbohydrate	Pentose Metabolism
arabitol/xylitol	0.24399945	1.06E-07	Carbohydrate	Pentose Metabolism
ribonate (ribonolactone)	0.242901624	1.40E-09	Carbohydrate	Pentose Metabolism
ribulonate/xylulonate*	0.199004805	6.84E-06	Carbohydrate	Pentose Metabolism
arabinose	0.195101787	2.43E-07	Carbohydrate	Pentose Metabolism
xylose	0.142342029	1.27E-04	Carbohydrate	Pentose Metabolism
sedoheptulose	0.134110627	6.38E-03	Carbohydrate	Pentose Metabolism
N2,N2-dimethyl guanosine	0.338920912	2.02E-09	Nucleotide	Purine Metabolism
1-methyladenosine	0.171469181	1.40E-08	Nucleotide	Purine Metabolism
acetylcarnitine (C2)	0.139843652	1.15E-03	Lipid	Short-chain Acylcarnitine
malonyl carnitine (C3-DC)	0.201698192	5.21E-06	Lipid	Short-chain Acylcarnitine

3-hydroxybutyrylcarnitine (C3-DC)	0.191185584	3.13E-04	Lipid	Short-chain Acylcarnitine
propionylcarnitine (C3)	0.139516903	4.57E-03	Lipid	Short-chain Acylcarnitine
2-methyl malonyl carnitine (C4-DC)	0.312976363	4.55E-08	Lipid	Short-chain Acylcarnitine
succinyl carnitine (C4-DC)	0.210904338	4.02E-06	Energy	Short-chain Acylcarnitine
iso butyryl carnitine (C4)	0.18255846	2.14E-03	Amino Acid	Short-chain Acylcarnitine
butyryl carnitine (C4)	0.132588051	1.74E-02	Lipid	Short-chain Acylcarnitine
tiglyl carnitine (C5)	0.215073761	2.36E-05	Amino Acid	Short-chain Acylcarnitine
glutaroylcarnitine (C5)	0.186774719	1.50E-04	Amino Acid	Short-chain Acylcarnitine
2-methylbutyroylcarnitine (C5)	0.177754615	1.05E-03	Amino Acid	Short-chain Acylcarnitine
isovalerylcarnitine (C5)	0.137011526	7.71E-03	Amino Acid	Short-chain Acylcarnitine
3-methylglutarylcarnitine (C6-DC)	0.280232266	8.38E-06	Amino Acid	Short-chain Acylcarnitine
adipoylcarnitine (C6-DC)	0.262247993	8.25E-06	Lipid	Short-chain Acylcarnitine
hexanoylcarnitine (C6)	0.177983823	4.57E-04	Lipid	Short-chain Acylcarnitine
3-methyladipoylcarnitine (C7-DC)	0.32397815	1.09E-08	Lipid	Short-chain Acylcarnitine
sphingomyelin (d18:2/24:2)*	-0.078102737	4.50E-02	Lipid	Sphingomyelins
sphingomyelin (d18:1/22:1, d18:2/22:0, d16:1/24:1)*	-0.096197859	2.24E-03	Lipid	Sphingomyelins
sphingomyelin (d18:1/17:0, d17:1/18:0, d19:1/16:0)	-0.101738087	4.15E-03	Lipid	Sphingomyelins
sphingomyelin (d18:2/18:1)*	-0.103544478	3.50E-03	Lipid	Sphingomyelins
behenoyl sphingomyelin (d18:1/22:0)*	-0.111076338	3.17E-04	Lipid	Sphingomyelins
lignoceroyl sphingomyelin (d18:1/24:0)	-0.114023601	1.70E-03	Lipid	Sphingomyelins
stearoyl sphingomyelin (d18:1/18:0)	-0.11647932	8.27E-04	Lipid	Sphingomyelins
sphingomyelin (d18:2/21:0, d16:2/23:0)*	-0.118326289	3.70E-03	Lipid	Sphingomyelins
sphingomyelin (d18:2/23:0, d18:1/23:1, d17:1/24:1)*	-0.12087178	3.19E-03	Lipid	Sphingomyelins
sphingomyelin (d18:1/20:0, d16:1/22:0)*	-0.122978034	1.75E-04	Lipid	Sphingomyelins
sphingomyelin (d18:1/18:1, d18:2/18:0)	-0.137596005	5.91E-05	Lipid	Sphingomyelins
sphingomyelin (d18:1/20:1, d18:2/20:0)*	-0.139095079	9.72E-05	Lipid	Sphingomyelins

sphingomyelin (d18:1/25:0, d19:0/24:1, d20:1/23:0, d19:1/24:0)*	-0.140129631	1.04E-03	Lipid	Sphingomyelins
sphingomyelin (d18:1/19:0, d19:1/18:0)*	-0.146092668	2.85E-04	Lipid	Sphingomyelins
sphingomyelin (d18:1/21:0, d17:1/22:0, d16:1/23:0)*	-0.158814217	3.36E-04	Lipid	Sphingomyelins
tricosanoyl sphingomyelin (d18:1/23:0)*	-0.160802384	3.04E-05	Lipid	Sphingomyelins

Note: Significant results were presented following individual mixed effects modeling of each of the 983 individual metabolites measured at day 0, 3, and 7. All estimates were adjusted for age, sex, SAPS II, admission diagnosis, 25(OH)D at randomization, absolute change in 25(OH)D level at day 3, plasma day, and individual patient (as the random-intercept). A multiple test-corrected thresholds of $q < 0.05$ was used to identify all significant associations. Positive β coefficient values indicate higher metabolite abundance with uCCI ≥ 4 relative to those with uCCI < 4.

Figure 1: Survival analysis for uCCI groups

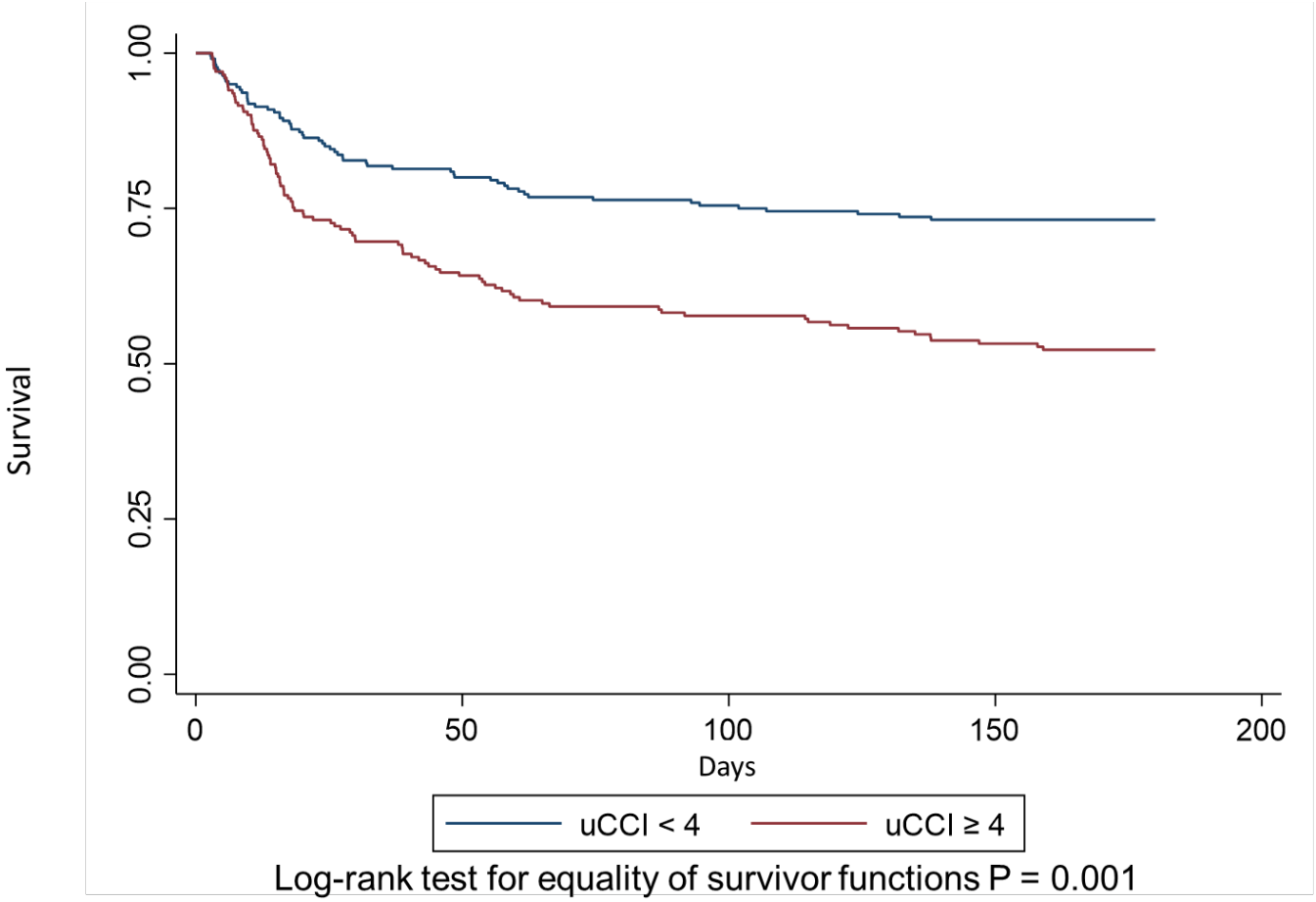

Figure 2. Day 0 OPLS-DA

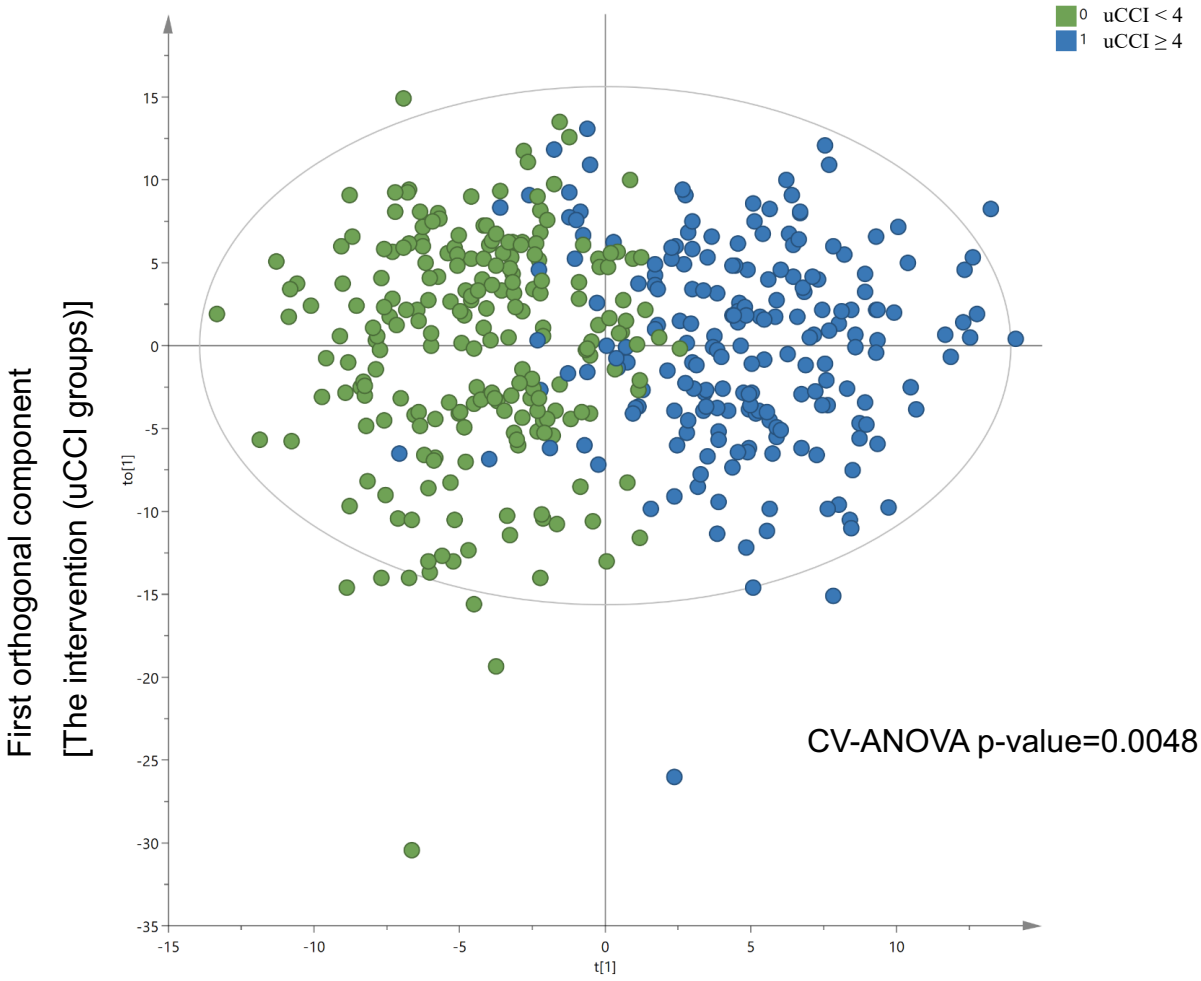

The predictive component (Metabolites at Day 0)

Supplementary Table S1. Cohort Comorbidities

Comorbidity	uCCI<4	uCCI≥4	Total
Congestive heart failure No. (%)	66 (30.00)	100 (49.75)	166 (39.43)
Dementia No. (%)	2 (0.91)	5 (2.49)	7 (1.66)
Chronic pulmonary disease No. (%)	21 (9.55)	49 (24.38)	70 (16.63)
Rheumatic disease No. (%)	6 (2.73)	6 (2.99)	12 (2.85)
Mild liver disease No. (%)	0 (0)	51 (25.37)	51 (12.11)
Diabetes with chronic complication No. (%)	27 (12.27)	52 (25.87)	79 (18.76)
Hemiplegia or paraplegia No. (%)	1 (0.45)	5 (2.49)	6 (1.43)
Renal disease No. (%)	0 (0)	116 (57.71)	116 (27.55)
Any malignancy without metastasis No. (%)	8 (3.64)	38 (1.89)	46 (10.92)
Moderate or severe liver disease No. (%)	0 (0)	26 (12.94)	26 (6.18)
Metastatic solid tumor No. (%)	0 (0)	2 (1.00)	2 (0.48)
AIDS No. (%)	0 (0)	0 (0)	0 (0)

Supplemental Figure 1. Consort flow diagram

Manuscript # 2

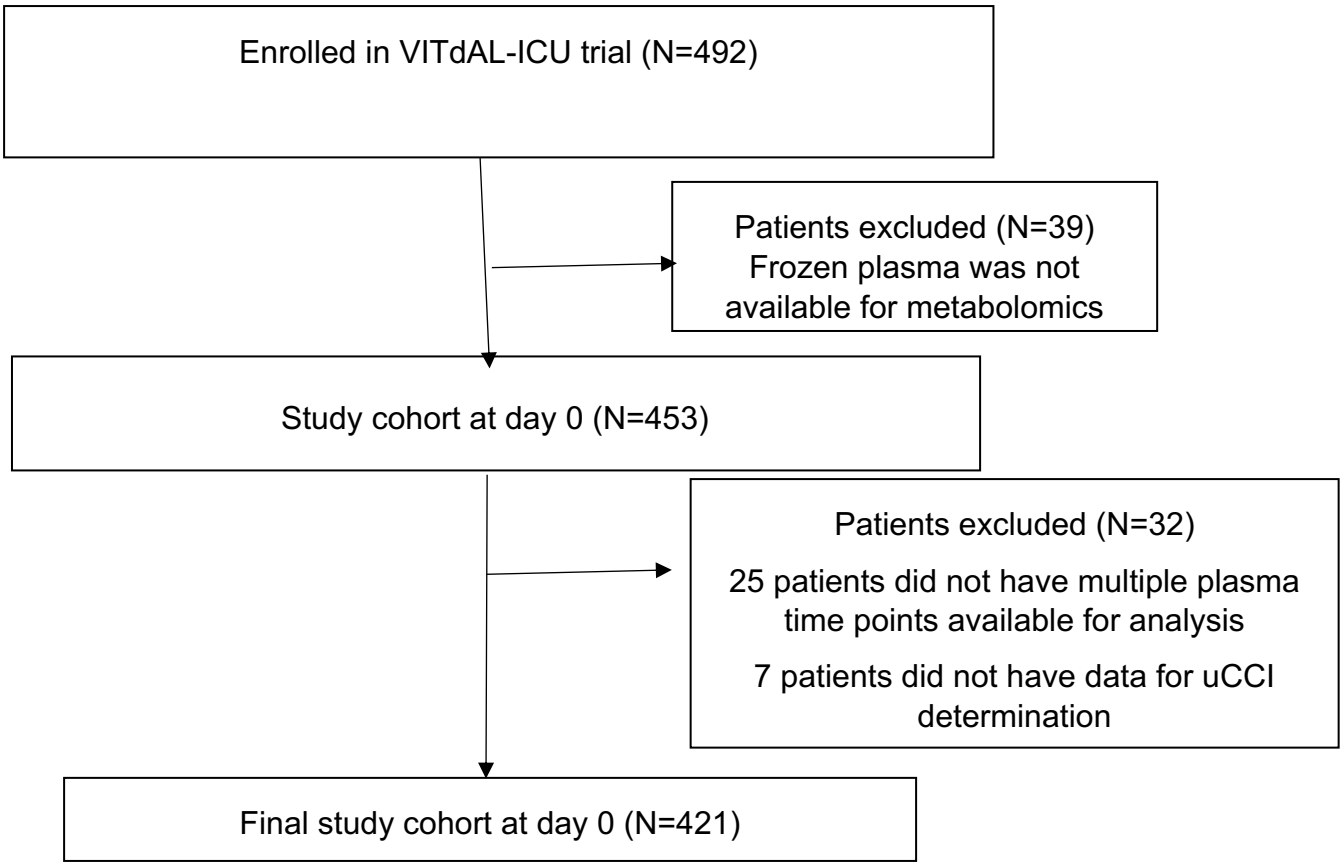

References

1. Maslove DM, Tang B, Shankar-Hari M, Lawler PR, Angus DC, Baillie JK, et al. Redefining critical illness. Nature medicine. 2022;28(6):1141-8.
2. Esper AM, Martin GS. The impact of comorbid [corrected] conditions on critical illness. Crit Care Med. 2011;39(12):2728-35.
3. McPeake J, Quasim T, Henderson P, Leyland AH, Lone NI, Walters M, et al. Multimorbidity and Its Relationship With Long-Term Outcomes After Critical Care Discharge: A Prospective Cohort Study. Chest. 2021;160(5):1681-92.
4. Kiehntopf M, Nin N, Bauer M. Metabolism, metabolome, and metabolomics in intensive care: is it time to move beyond monitoring of glucose and lactate? Am J Respir Crit Care Med. 2013;187(9):906-7.
5. Kobayashi H, Amrein K, Lasky-Su J, Christopher KB. Procalcitonin Metabolomics in the Critically Ill reveal relationships between inflammation intensity and energy utilization pathways. Scientific Reports. 2021;11:23194.
6. Ashrafian H, Sounderajah V, Glen R, Ebbels T, Blaise BJ, Kalra D, et al. Metabolomics: The Stethoscope for the Twenty-First Century. Med Princ Pract. 2021;30(4):301-10.
7. Klassen A, Faccio AT, Canuto GA, da Cruz PL, Ribeiro HC, Tavares MF, et al. Metabolomics: Definitions and Significance in Systems Biology. Adv Exp Med Biol. 2017;965:3-17.
8. Wishart DS, Jewison T, Guo AC, Wilson M, Knox C, Liu Y, et al. HMDB 3.0--The Human Metabolome Database in 2013. Nucleic acids research. 2013;41(Database issue):D801-7.
9. Quan H, Li B, Couris CM, Fushimi K, Graham P, Hider P, et al. Updating and validating the Charlson comorbidity index and score for risk adjustment in hospital discharge abstracts using data from 6 countries. Am J Epidemiol. 2011;173(6):676-82.
10. Ternavasio-de la Vega HG, Castano-Romero F, Ragozzino S, Sanchez Gonzalez R, Vaquero-Herrero MP, Siller-Ruiz M, et al. The updated Charlson comorbidity index is a useful predictor of mortality in patients with Staphylococcus aureus bacteraemia. Epidemiol Infect. 2018;146(16):2122-30.
11. Heng JS, Clancy O, Atkins J, Leon-Villapalos J, Williams AJ, Keays R, et al. Revised Baux Score and updated Charlson comorbidity index are independently associated with mortality in burns intensive care patients. Burns. 2015;41(7):1420-7.
12. Wernerman J, Christopher KB, Annane D, Casaer MP, Coopersmith CM, Deane AM, et al. Metabolic support in the critically ill: a consensus of 19. Crit Care. 2019;23(1):318.
13. Amrein K, Schnedl C, Holl A, Riedl R, Christopher KB, Pachler C, et al. Effect of high-dose vitamin D3 on hospital length of stay in critically ill patients with vitamin D deficiency: the VITdAL-ICU randomized clinical trial. JAMA. 2014;312(15):1520-30.
14. World Medical A. World Medical Association Declaration of Helsinki: ethical principles for medical research involving human subjects. JAMA. 2013;310(20):2191-4.
15. van den Berg RA, Hoefsloot HC, Westerhuis JA, Smilde AK, van der Werf MJ. Centering, scaling, and transformations: improving the biological information content of metabolomics data. BMC Genomics. 2006;7:142.

16. Struja T, Eckart A, Kutz A, Huber A, Neyer P, Kraenzlin M, et al. Metabolomics for Prediction of Relapse in Graves' Disease: Observational Pilot Study. Front Endocrinol (Lausanne). 2018;9:623.
17. Parisi LR, Li N, Atilla-Gokcumen GE. Very Long Chain Fatty Acids Are Functionally Involved in Necroptosis. Cell Chem Biol. 2017;24(12):1445-54 e8.
18. Kaplan E, Meier P. Nonparametric estimation from incomplete observations. J AM Stat Assn. 1958;53:457-81.
19. Mantel N. Evaluation of survival data and two new rank order statistics arising in its consideration. Cancer Chemother Rep. 1966;50(3):163-70.
20. van Iterson M, t Hoen PA, Pedotti P, Hooiveld GJ, den Dunnen JT, van Ommen GJ, et al. Relative power and sample size analysis on gene expression profiling data. BMC Genomics. 2009;10:439.
21. Chong J, Xia J. Using MetaboAnalyst 4.0 for Metabolomics Data Analysis, Interpretation, and Integration with Other Omics Data. Methods Mol Biol. 2020;2104:337-60.
22. FitzMaurice GM, Laird NM, Ware JH. Applied longitudinal analysis. Hoboken, New Jersey: Wiley; 2011.
23. Benjamini Y, Hochberg Y. Controlling for false discovery rate: a practical and powerful approach to multiple testing. Journal of the Royal Statistical Society Series B (Methodological). 1995;57:289–300.
24. Matthew B, William R. Partial least squares for discrimination. Journal of Chemometrics. 2003;17(3):166-73.
25. Worley B, Powers R. PCA as a practical indicator of OPLS-DA model reliability. Curr Metabolomics. 2016;4(2):97-103.
26. Westerhuis JA, Hoefsloot HCJ, Smit S, Vis DJ, Smilde AK, van Velzen EJJ, et al. Assessment of PLSDA cross validation. Metabolomics 2008;4(1):81–9.
27. Eriksson L, Trygg J, Wold S. CV-ANOVA for significance testing of PLS and OPLS models. Journal of Chemometrics. 2008;22(11-12):594-600.
28. StataCorp. Stata Statistical Software: Release 16. College Station, TX: StataCorp LP.; 2019.
29. Westerhuis JA, Hoefsloot HCJ, Smit S, Vis DJ, Smilde AK, van Velzen EJJ, et al. Assessment of PLSDA cross validation. Metabolomics. 2008;4(1):81-9.
30. Shalom-Barak T, Knaus UG. A p21-activated kinase-controlled metabolic switch up-regulates phagocyte NADPH oxidase. J Biol Chem. 2002;277(43):40659-65.
31. Costa CG, Struys EA, Bootsma A, ten Brink HJ, Dorland L, Tavares de Almeida I, et al. Quantitative analysis of plasma acylcarnitines using gas chromatography chemical ionization mass fragmentography. J Lipid Res. 1997;38(1):173-82.
32. Koves TR, Ussher JR, Noland RC, Slentz D, Mosedale M, Ilkayeva O, et al. Mitochondrial overload and incomplete fatty acid oxidation contribute to skeletal muscle insulin resistance. Cell Metab. 2008;7(1):45-56.
33. Newgard CB. Interplay between lipids and branched-chain amino acids in development of insulin resistance. Cell Metab. 2012;15(5):606-14.
34. Schöch G, Topp H, Held A, Heller-Schöch G, Ballauff A, F. M, et al. Interrelation between whole-body turnover rates of RNA and protein. Eur J Clin Nutr. 1990;44(9):647-58.

35. Sander G, Topp H, Heller-Schoch G, Wieland J, Schoch G. Ribonucleic acid turnover in man:RNA catabolites in urine as measure for the metabolism of each of the three major species of RNA. Clin Sci (Lond). 1986;71(4):367-74.
36. Kirchner S, Ignatova Z. Emerging roles of tRNA in adaptive translation, signalling dynamics and disease. Nature reviews Genetics. 2015;16(2):98-112.
37. Mishima E, Inoue C, Saigusa D, Inoue R, Ito K, Suzuki Y, et al. Conformational change in transfer RNA is an early indicator of acute cellular damage. J Am Soc Nephrol. 2014;25(10):2316-26.
38. Ottosson F, Smith E, Fernandez C, Melander O. Plasma Metabolites Associate with All-Cause Mortality in Individuals with Type 2 Diabetes. Metabolites. 2020;10(8).
39. Kletzien RF, Harris PK, Foellmi LA. Glucose-6-phosphate dehydrogenase: a "housekeeping" enzyme subject to tissue-specific regulation by hormones, nutrients, and oxidant stress. FASEB J. 1994;8(2):174-81.
40. Kruger A, Gruning NM, Wamelink MM, Kerick M, Kirpy A, Parkhomchuk D, et al. The pentose phosphate pathway is a metabolic redox sensor and regulates transcription during the antioxidant response. Antioxid Redox Signal. 2011;15(2):311-24.
41. Haji-Michael PG, Ladriere L, Sener A, Vincent JL, Malaisse WJ. Leukocyte glycolysis and lactate output in animal sepsis and ex vivo human blood. Metabolism. 1999;48(6):779-85.
42. Nalos M, Parnell G, Robergs R, Booth D, McLean AS, Tang BM. Transcriptional reprogramming of metabolic pathways in critically ill patients. Intensive Care Med Exp. 2016;4(1):21.
43. Taniguchi M, Okazaki T. The role of sphingomyelin and sphingomyelin synthases in cell death, proliferation and migration-from cell and animal models to human disorders. Biochim Biophys Acta. 2014;1841(5):692-703.
44. Yabu T, Shiba H, Shibasaki Y, Nakanishi T, Imamura S, Touhata K, et al. Stress-induced ceramide generation and apoptosis via the phosphorylation and activation of nSMase1 by JNK signaling. Cell death and differentiation. 2015;22(2):258-73.
45. Vickers AJ. How many repeated measures in repeated measures designs? Statistical issues for comparative trials. BMC Med Res Methodol. 2003;3:22.
46. Frison L, Pocock SJ. Repeated measures in clinical trials: analysis using mean summary statistics and its implications for design. Stat Med. 1992;11(13):1685-704.
47. Kobayashi H, Amrein K, Lasky-Su JA, Christopher KB. Procalcitonin metabolomics in the critically ill reveal relationships between inflammation intensity and energy utilization pathways. Sci Rep. 2021;11(1):23194.
48. Fang H, Brooks GP, Rizzo ML, Espy KA, Barcikowski RS. A Monte Carlo Power Analysis of Traditional Repeated Measures and Hierarchical Multivariate Linear Models in Longitudinal Data Analysis. J Mod Appl Stat Methods. 2008;7(1).
49. Kelly RS, Croteau-Chonka DC, Dahlin A, Mirzakhani H, Wu AC, Wan ES, et al. Integration of metabolomic and transcriptomic networks in pregnant women reveals biological pathways and predictive signatures associated with preeclampsia. Metabolomics. 2017;13(1).
50. Lee-Sarwar K, Kelly RS, Lasky-Su J, Kachroo P, Zeiger RS, O'Connor GT, et al. Dietary and Plasma Polyunsaturated Fatty Acids Are Inversely Associated with Asthma and Atopy in Early Childhood. J Allergy Clin Immunol Pract. 2019;7(2):529-38 e8.

51. Mei Y, Kim BS, Tsui K. Linear mixed effects models for feature selection in high dimensional NMR spectra. Exprt Syst Applic. 2009;36:4703–8.
52. Ernest B, Gooding JR, Campagna SR, Saxton AM, Voy BH. MetabR: an R script for linear model analysis of quantitative metabolomic data. BMC Res Notes. 2012;5:596.
53. Chary S, Amrein K, Mahmoud SH, Lasky-Su JA, Christopher KB. Sex-Specific Catabolic Metabolism Alterations in the Critically Ill following High Dose Vitamin D. Metabolites. 2022;12(3).
54. Dunn WB, Lin W, Broadhurst D, Begley P, Brown M, Zelena E, et al. Molecular phenotyping of a UK population: defining the human serum metabolome. Metabolomics. 2015;11(1):9-26.

SUMMARY OF MANUSCRIPT 1 AND MANUSCRIPT 2 CONCLUSIONS

This work depicted two critical-care VITdAL-ICU metabolomics studies. Two ICU studies found different plasma metabolomics responses to hyperglycemia and chronic comorbidities (ICUs).

In Manuscript 1, Based on longitudinal metabolomics data and mixed-effect linear regression analysis, we found 84 metabolites had significantly positive (q-value <0.05) associations with serum glucose, dominated by increases in diacylglycerol (DAG) species, branched-chain amino acids (BCAAs), and glycerophospholipid species (phosphatidylcholine, phosphatidylethanolamine, and phosphatidylinositol) and including plasma glucose, alanine, and lactate. These metabolic profile alterations indicate that energy utilization is altered in critically ill hyperglycemic patients, explicitly indicating a metabolic shift involving mitochondria and the endoplasmic reticulum.

In Manuscript 2, we found 430 metabolites strongly associated with uCCI<4 or uCCI>4. In repeated measure metabolomics data, several metabolites increased with increasing uCCI, including BCAA, short-chain acylcarnitines, purine nucleotides (1-methyladenosine (m1A), N2, N2-dimethyl guanosine (m22G), and pentose phosphate pathway activation. In contrast, others decreased, such as Sphingomyelin. Alteration of these metabolic pathways associated with comorbidities indicates chronic diseases are related to differential utilization of energy pathways among critically ill patients.

OVERALL DISCUSSION AND PERSPECTIVES

Our present study approach has multiple strengths. First, repeated plasma sample measurements in individual patients increase our study's statistical power. We used linear mixed–effect models to remove confounding variables with a fixed effect (age, SAPS II, etc.) and a random effect (plasma sampling day). Importantly, by adjusting for the absolute change in 25(OH)D level at day 0, 3, and 7, we mitigate the effect of the trial intervention on the observed metabolomic changes associated with hyperglycemia.

Potential limitations exist in our study. First, since the subjects were recruited from a single large academic medical center, our cohort may not be generalizable to all critically ill patients. Second, despite the multivariable adjustment, we could not exclude the effect of unknown confounders due to nonrandomized metabolite abundance comparisons. Third, subject data is absent for HbA1C, parenteral nutrition, dextrose use, and dose and duration of medications that can contribute to elevated glucose. Lastly, as our study is post-hoc, our inferences require external validation and should be considered hypothesis-generating.

Critical illnesses have many clinical risk parameters and pathophysiological factors that no single biomarker can capture. Metabolomics platforms and technology can support clinical decisions and patient-centered care in routine clinical practice. It will explain complex disease pathophysiology and advance precision medicine.